

University of Windsor

Scholarship at UWindor

Electronic Theses and Dissertations

Theses, Dissertations, and Major Papers

2004

Robust control for an electric power steering system.

Ke Li

University of Windsor

Follow this and additional works at: <https://scholar.uwindsor.ca/etd>

Recommended Citation

Li, Ke, "Robust control for an electric power steering system." (2004). *Electronic Theses and Dissertations*. 3355.

<https://scholar.uwindsor.ca/etd/3355>

This online database contains the full-text of PhD dissertations and Masters' theses of University of Windsor students from 1954 forward. These documents are made available for personal study and research purposes only, in accordance with the Canadian Copyright Act and the Creative Commons license—CC BY-NC-ND (Attribution, Non-Commercial, No Derivative Works). Under this license, works must always be attributed to the copyright holder (original author), cannot be used for any commercial purposes, and may not be altered. Any other use would require the permission of the copyright holder. Students may inquire about withdrawing their dissertation and/or thesis from this database. For additional inquiries, please contact the repository administrator via email (scholarship@uwindsor.ca) or by telephone at 519-253-3000ext. 3208.

Robust Control for an Electric Power Steering System

by
Ke Li

A Thesis

Submitted to the Faculty of Graduate Studies and Research
through Electrical Engineering
In Partial Fulfillment of the Requirements for
The Degree of Master of Applied Science at the
University of Windsor

Windsor, Ontario, Canada

2004

© 2004 Ke Li



Library and
Archives Canada

Bibliothèque et
Archives Canada

Published Heritage
Branch

Direction du
Patrimoine de l'édition

395 Wellington Street
Ottawa ON K1A 0N4
Canada

395, rue Wellington
Ottawa ON K1A 0N4
Canada

Your file *Votre référence*

ISBN: 0-494-00162-3

Our file *Notre référence*

ISBN: 0-494-00162-3

NOTICE:

The author has granted a non-exclusive license allowing Library and Archives Canada to reproduce, publish, archive, preserve, conserve, communicate to the public by telecommunication or on the Internet, loan, distribute and sell theses worldwide, for commercial or non-commercial purposes, in microform, paper, electronic and/or any other formats.

The author retains copyright ownership and moral rights in this thesis. Neither the thesis nor substantial extracts from it may be printed or otherwise reproduced without the author's permission.

AVIS:

L'auteur a accordé une licence non exclusive permettant à la Bibliothèque et Archives Canada de reproduire, publier, archiver, sauvegarder, conserver, transmettre au public par télécommunication ou par l'Internet, prêter, distribuer et vendre des thèses partout dans le monde, à des fins commerciales ou autres, sur support microforme, papier, électronique et/ou autres formats.

L'auteur conserve la propriété du droit d'auteur et des droits moraux qui protègent cette thèse. Ni la thèse ni des extraits substantiels de celle-ci ne doivent être imprimés ou autrement reproduits sans son autorisation.

In compliance with the Canadian Privacy Act some supporting forms may have been removed from this thesis.

Conformément à la loi canadienne sur la protection de la vie privée, quelques formulaires secondaires ont été enlevés de cette thèse.

While these forms may be included in the document page count, their removal does not represent any loss of content from the thesis.

Bien que ces formulaires aient inclus dans la pagination, il n'y aura aucun contenu manquant.


Canada

1018246

Robust Control for an Electric Power Steering System

by

Ke Li

APPROVED BY:

N. Kar, Chair

Electrical and Computer Engineering

G. Zhang

Industrial and Manufacturing Systems Engineering

B. Shahrrava

Electrical and Computer Engineering

X. Chen, Advisor

Electrical and Computer Engineering

September 21, 2004

ABSTRACT

The EPS (electric power steering) system is one of the safety-critical systems in modern automotive control system. Various control algorithms are derived in order to achieve the specified system characters. Steering feel is effectively defined the steering wheel torque, or reaction torque, the driver senses during steering maneuvers and by the vehicle response to the steering inputs. A favourable steering feel can be formulated in frequency domain. Most of the essential information from road is in low frequency domain, while the road torque in high frequency domain can be treated as disturbance.

Most of these existing controllers use the controller architecture as motor control plus compensators. This controller architecture has its own limitation because the controller, which is located in the motor feedback control loop, is not sensitive to the signals, which is in steering feedback loop. It is difficult to design a robust controller based on this controller architecture.

In this thesis, a dynamic model for an EPS system was derived. And then, new controller architecture with an extra logical controller in the steering feedback loop, called motion controller, was proposed to increase the sensitivity of the control system to the system. Finally, a robust control system was designed based on the proposed EPS model and the new controller architecture.

The disturbance signal is the high frequency part of the torque from road to the rack and pinion. The disturbance can be modeled as bounded noise or white noise. H_∞ technology is often used to attenuate the bounded noise. The control design was divided into two stages. The first stage is to design a PI motor controller to increase the reaction speed. The next stage is to design an H_∞ motion controller based on the frequency character of the disturbance signal.

Simulations were carried out to demonstrate the controller's performance and robustness characteristics for both bounded noise and white noise. The results of these simulations indicate that, to compare with the traditional control system, the proposed controller provides better noise attenuation for bounded noise but provides worse performance for white noise.

ACKNOWLEDGEMENTS

I would like to acknowledge my deepest gratitude and indebtedness to **Dr. Xiang Chen**, Associate Professor, Department of Electrical and Computer Engineering, University of Windsor, for his keen interest in the research and his encouragement, sincere guidance, friendly supervision, valuable suggestion and financial support at every stage of my work. Without his continuous help, this research would not be possible to be accomplished. So I wish to express my special thanks and respect to **Dr. Xiang Chen**.

I was fortunate to have an exceptional external advisor. **Dr. Shaotang Chen**, CTO of VCF tech. Inc., has provided financial support, invaluable insight, practical advice and much needed mentorship.

In addition, I also would like to thank to **Dr. Behnam Shahrava**, as internal reader from the Department of Electrical and Computer Engineering as well as **Dr. Guoqing Zhang**, as external reader from the Department of Industrial and Manufacturing Systems for their valuable suggestions during the evaluation of this thesis and the seminars.

Lastly, I wish to thank my co-workers, both in University of Windsor and VCF tech. Inc. for their continuous support and encouragement during the entire progress of the work.

Thank you.

TABLE OF CONTENTS

ABSTRACT	III
ACKNOWLEDGEMENTS	IV
LIST OF TABLES	IX
LIST OF FIGURES	X
ABBREVIATION	XII
CHAPTER 1: INTRODUCTION	1
1.1 INTRODUCTION	1
1.2 LITERATURE SURVEY ON MODELING AND CONTROL OF EPS SYSTEM	1
1.2.1 DYNAMIC MODELING SURVEY	2
1.2.2 CONTROL DESIGN SURVEY	4
1.3 MOTIVATION AND OBJECTIVE	9
1.4 CONTRIBUTION	10
1.4.1 EPS MODEL DERIVATION	11
1.4.2 NEW CONTROLLER ARCHITECTURE	11
1.4.3 ROBUST CONTROL SYSTEM DESIGN	11
1.5 THESIS OVERVIEW	12
CHAPTER 2: PRELIMINARY THEORY	13
2.1 VECTOR NORMS AND MATRIX NORMS	13
2.2 ROBUST AND OPTIMAL CONTROL THEORY	14
2.3 H_{∞} CONTROLLER DESIGN	16
2.3.1 STATE FEEDBACK DESIGN	17
2.3.2 OUTPUT FEEDBACK DESIGN	17

2.3.3	H_{∞} SYNTHESIS USING MATLAB™	18
2.3.4	PLANT AUGMENTATION	20
2.4	SINGULAR-VALUE LOOP SHAPING	22
CHAPTER 3: EPS DYNAMIC MODEL		26
3.1	INTRODUCTION	26
3.2	THE GENERAL DESCRIPTION OF AN EPS SYSTEM	26
3.3	COMPONENT-WISE DYNAMIC MODEL	28
3.3.1	STEERING WHEEL DYNAMIC MODEL	28
3.3.2	TORQUE SENSOR DYNAMIC MODEL	28
3.3.3	THE DYNAMIC MODEL OF A BRUSHED DC MOTOR	29
3.3.4	THE DYNAMIC MODEL OF PINION AND RACK ASSEMBLY	30
3.4	THE DYNAMIC MODEL OF AN EPS SYSTEM	31
3.5	MODEL VERIFICATION	32
3.5.1	SYSTEM STABILITY ANALYSIS	33
3.5.2	VIRTUAL VEHICLE MODULE	33
3.5.3	SIMULATION DESCRIPTION	34
3.5.4	SIMULATION RESULTS AND DISCUSSION	35
3.5.5	CONCLUSION	41
CHAPTER 4: TWO-DEGREE FREEDOM CONTROLLER DESIGN		42
4.1	INTRODUCTION	42
4.2	DESIGN SPECIFICATIONS	42
4.3	SYSTEM MODEL	43
4.3.1	BLOCK DIAGRAM	43
4.3.2	STATE SPACE MODEL	44
4.4	NEW CONTROLLER ARCHITECTURE	45
4.5	MOTOR CONTROLLER DESIGN	47

4.5.1	MOTOR CONTROL SYSTEM DESCRIPTION	47
4.5.2	PI CONTROLLER DESIGN	47
4.6	H_{∞} CONTROLLER DESIGN	48
4.6.1	SYSTEM AUGMENTATION	48
4.6.2	H_{∞} CONTROL SYNTHESIS	50
4.7	STABILITY ANALYSIS	52
4.8	DISCUSSION AND CONCLUSION	53
4.9	PID MOTION CONTROLLER	54
CHAPTER 5: SIMULATION		57
5.1	INTRODUCTION	57
5.2	TESTBENCH	57
5.3	SIMULATION RESULT DESCRIPTION	58
5.4	RESULT DISCUSSION	66
5.4.1	BOUNDED NOISE	66
5.4.2	WHITE NOISE	67
5.5	PID MOTION CONTROLLER SIMULATION	67
CHAPTER 6: CONCLUSIONS		71
6.1	INTRODUCTION	71
6.2	DISCUSSION	71
6.3	FUTURE WORK	71
6.3.1	IMPLEMENTATION	72
6.3.1.1	EXPERIMENTAL SETUP	72
6.3.1.2	REAL TIME VIRTUAL VEHICLE SETUP	73
6.3.1.3	CONTROLLER	73
6.3.1.4	PC	74
6.3.2	ORDER REDUCTION	74

6.3.3	MOTOR CONTROL ALGORITHM	74
6.3.4	VARIABLE ASSIST CONTROL	74
6.3.5	WHITE NOISE ATTENUATION	74
CHAPTER 7: BIBLIOGRAPHY		76
VITA AUCTORIS		80

LIST OF TABLES

Table 3-1: the input/output signals of each module	34
Table 3-2: the configuration of the target vehicle	35
Table 5-1: three control strategies and simulation configurations	58
Table 5-2: the shown simulation results from Figure 5-2 to Figure 5-7.	59

LIST OF FIGURES

Figure 2-1: H_{∞} synthesis using MatLab	19
Figure 2-2: Plant Augmentation	21
Figure 2-3: Traditional Feedback Control System	22
Figure 2-4: Additive/Multiplicative uncertainty.	24
Figure 3-1: Three Types of Integrated Systems	26
Figure 3-2: EPS Schematic Arrangement.	27
Figure 3-3: Presented EPS Dynamic Model	32
Figure 3-4: The Testbench and the System Input Signal	37
Figure 3-5: the Time Domain Response of the Steering Wheel	38
Figure 3-6: The Comparison Between the Angles of the Front Road Wheels	39
Figure 3-7: The torque on rack and pinion generated from front wheels	40
Figure 3-8: The response of the vehicle speed	41
Figure 4-1: EPS System Block Diagram	43
Figure 4-2: New Control Architecture With Motion Controller	46
Figure 4-3: Motor Control Assembly	46
Figure 4-4: Controlled Plant	46
Figure 4-5: the Step Response with Two PI Controllers	48
Figure 4-6: Plant Augmentation	49
Figure 4-7: Weighting Strategy	50
Figure 4-8: γ -iteration output	51
Figure 4-9: successful H_{∞} Control Synthesis	51
Figure 4-10: Bode diagram for the frequency characteristics from road wheel torque to reaction torque.	54
Figure 4-11: using PD motion controller	56
Figure 4-12: Using PI Motion Controller	56
Figure 5-1: Simulation Testbench	57
Figure 5-2: Zero Mean Random Number Noise with Variance = 100	60
Figure 5-3: Zero-mean Random Number Noise with Variance = 50	61

Figure 5-4: Zero-Mean Random Number Noise with Variance = 20	62
Figure 5-5: White Noise with Power = 10	63
Figure 5-6: White Noise with Power = 1	64
Figure 5-7: White Noise with Power = 0.1	65
Figure 5-8: Simulation of PID Motion Controller System - 1	68
Figure 5-9: Simulation of PID Motion Controller System - 2	69
Figure 5-10: Simulation of PID Motion Controller System - 3	70
Figure 6-1: Experimental Setup for Controller Test Implementation	72

ABBREVIATION

BDC	Brushed DC
BLDC	Brushless DC
CAN	Controller Area Network
DSP	Digital Signal Processor
EPS	Electric Power Steering
HYPAS	Hydraulic Power Assist Steering
LMI	linear matrix inequalities
LQG	linear quadratic gaussian
LQR	linear quadratic regulator
MIMO	multi-input and multi-output
MMR	moment restraints
PS	Power Steering
RWP	Road Wheel Position measured in degree
RWT	The torque from road wheel to rack and pinion, measured in Nm
TDF	Two-degree Freedom
TRT	The reaction torque, which is the torque sensor output, measured in Nm

CHAPTER 1:INTRODUCTION

1.1 INTRODUCTION

Drivers will expect continual improvement in driving safety and comfort. The steering column has a direct relationship with vehicle manoeuvring, a basic function of the automobile, and is thus specified as a safety-critical automobile part. Steering columns need to satisfy various requirements, such as collision safety, steering feeling (column rigidity), and antitheft (key lock strength) performance.

Growing needs for safety and environmental friendliness have led to intense development of new steering column-related technologies, in particular, those regarding electric power steering systems. The development of the steering column, which is the vital part of the overall steering system, must keep pace with these advances. Also, column manufacturers must introduce new column designs and production technologies enabling low-cost columns in order to survive amidst severe cost competition today.

To compare with the hybrid-power assist steering system, an electric power steering (EPS) system promises weight reduction, fuel savings and package flexibility, at no cost penalty. An EPS system for a vehicle is known in which the torque output from an electric motor for generating assist steering effort is reduced by a gearbox in order to transmit proper torque and velocity to the output shaft of the steering system [2].

EPS represents the future of power-assisted steering technology for passenger cars and is already beginning to appear in high-volume, lead-vehicle applications [1]. More versatile than conventional hydraulic power-assist steering system (HYPAS), the essence of EPS is to provide steering assistance to the driver using an electrically controlled electric motor. EPS is a classic example of a smart actuator operating under feedback control.

1.2 LITERATURE SURVEY ON MODELING AND CONTROL OF EPS SYSTEM

In order to design a robust controller, a realistic dynamic model is needed to derive and design the appropriate controller with which the desired performance is achieved.

The issues of modeling and controller design are discussed in this section and a comprehensive literature survey is provided.

1.2.1 DYNAMIC MODELING SURVEY

In [4], a steering system retrofitted with an actuator is considered. The input and output of the steering system are the reference steering angle command to the actuator and the actual steering angle of the front wheel respectively. Open loop experimental data is fitted to a second order linear model.

Gary and Larry in General Motors modeled the vehicle power steering system as a feedback control system that hydraulically assists the driver in applying input steering commands to the vehicle [5]. If the rack is moving too slowly or too quickly, the valve will modulate the cylinder pressure to assist or hinder the motion. There is also a mechanical feed-forward path that directly connects the driver's input torque to the rack. Based on the concept of approaching power steering shudder from a control systems point of view introduced in [6], they derived the model equations. At the end of [5], specific analytical results that reveal the control/structure interaction are examined.

A. Zaremba and R. I. Davis presented dynamic analysis of a power assist steering system emphasis on system stability in [7]. The transfer functions that describe assist and steering system response, and driver's feel of the road are obtained in analytical form. To determine torque-speed requirements of the assist actuator, they chose zero and low speed parking and high-speed random steer conditions to investigate worst-case loads. A high level of steering assist can be a source of instability of the plant that results in vibration of a steering column and undesirable vehicle performance. Stability requirements are determined and critical parameters of assist design are obtained as a solution of the nonlinear equation that describes the boundary of the stability. The power gear is described as a dual-pinion arrangement, in which the driver input acts through one pinion and the power assist acts through another pinion. Using Lienard and Chipart criteria, they performed stability analysis and determined constraints on the maximum level of power assist that ensures all of the roots of dynamic system had negative real part.

In [8], the researchers from MIT propose a reduction model of a PS system. The model reduction procedure was introduced in [9]. In [8], the power steering system is modeled of two main units, namely a manual power transfer unit and a hydraulic power

assist unit. The manual unit consists of a steering wheel, a main shaft and a gear mechanism. The main parts of a hydraulic power steering system are: an oil pump, hoses and pipes, an oil reservoir, steering gear box that contains a pressure control valve, a rack and pinion mechanism, a piston and a power cylinder. Steering torque from the driver is transferred from the steering wheel to the pinion gear. The pressure control valve is placed between the main shaft and pinion gear, so that the valve moves corresponding to the input torque. The valve displacement from the neutral position produces an oil pressure change, and the pressure is guided to one of the cylinders corresponding to the valve movement direction. The pressure is converted to the force by the piston attached to the rack bar, and the force assist the driver to the front wheel.

Another reduced model introduced by Delphi is used to analyze various closed loop effects such as torque performance, disturbance rejection, noise rejection, road feel and stability [10]. The EPS system from Delphi, named E-Steer™, is made up of: a steering column, a gear assist mechanism attached to the column, a brushless DC (BLDC) motor, a controller and a sensor within the assist housing. The main purpose of the power steering system is to provide assist to the driver. This is achieved by the torque sensor, which measures the driver's torque and sends a signal to the controller proportional to the torque. The controller also receives steering position information from the position sensor that is collocated with the torque sensor and together they make up the sensor. The torque and position information is processed in the controller and an assist command is generated. This assist command is further modulated by the vehicle speed signal, which is also received by the controller. This command is given to the motor, which provides the torque to the assist mechanism. The gear mechanism amplifies this torque, and ultimately, the loop is closed by applying the assist torque to the steering column.

A complete and exhaustive dynamic model of EPS system would consist of all the masses and moments of inertia considered in relation to their interconnection with the various spring and damping elements that appear in the system. The fundamental behaviour of the system is dominated by low frequency mode. In [11], the dynamic model of a double-pinion type EPS is simplified by neglecting the stiff elements, which connect masses, because they contribute high frequency modes. That is to say, the model neglects

the masses of the tire rods and tires, tire motion, friction etc. and the inertias of power transforming elements, such as gears.

1.2.2 CONTROL DESIGN SURVEY

Various control algorithms are derived in order to achieve the specified system characteristics. The effectiveness of these designed controllers is then evaluated based on several factors, of which robust stability and robust performance are the most important. Stability is an indication of whether the system will reach a stable steady-state value, or will become unstable and crash. Performance refers to how well the system tracks any arbitrary reference trajectory. Robustness refers to how resilient the system is towards system parameters uncertainty and unexpected disturbances. In the course of the control action, it is necessary to measure and feedback the resulting system output, but this is not always possible in industry. Some quantities may not be easily measurable and/or it may be very costly to do so. Hence, in addition to having good performance and robustness, it is also desirable that the controller minimizes the number of feedbacks used.

A sliding mode controller cascaded by the frequency shaped optimal controller for drive by wire hydraulic power steering system utilizing sliding mode and exponentially convergent observers is presented in [12]. Using the robustness implications of the sliding mode control theory and the structure property of the hydraulic power steering system, a nonlinear controller cascaded by an optimal linear controller is designed to stabilize the steering system dynamics and track the steering wheel reference. The sliding mode controller works as an outer loop controller, which satisfies robust stabilization and reference tracking of the steering rack displacement state versus the bounded modeling parametric uncertainties. The frequency shaped optimal controller is proposed as an inner loop controller to satisfy reference tracking of the steering wheel angle.

The reference for the steering rack displacement is obtained to be proportional to the reference steering wheel angle. With this reference generation, all the nonlinearities caused by the gear and the other disturbances are omitted and an ideal reference rack displacement proportional to the steering wheel reference is derived for the steering rack dynamics.

The frequency shaped linear quadratic regulator (LQR) is used to track the desired steering wheel angle generated by the sliding mode controller while eliminating high frequency, high gain steering wheel torque.

Another controller for power steering system is designed using root locus method in [5]. The design by the root-locus method is based on reshaping the root locus of the system by adding poles and zeros to the system's open loop transfer function and forcing the root loci to pass through desired closed loop poles in the s plane. In [5], the system's close loop poles come from combination of the hydraulic, structure and mechanical dynamics. The position feedback root locus of a nominal vehicle system is derived and the stability margin is examined by using the Bode plot of the open loop transfer function.

Steering feel is effectively defined the steering wheel torque the driver senses during steering manoeuvres and by the vehicle response to the steering inputs. A number of papers [14], [15] and [16] attempted to qualify driver steering feel. Paper [13] addresses control synthesis and optimal performance issues in the design of EPS systems. The requirements of optimal steering dynamics can be naturally introduced as constraints in the control design. The first constraint is on the controller dc gain, which ensures the required level of steering torque amplification and proper functionality of the assist. The second constraint defines the maximum acceptable phase lag the controller can impose without noticeable consequences for steering feel. The third constraint is on pole and zero locations, which guarantees fast steering response.

The optimal controller synthesis is achieved by using the optimization routine in "optimization toolbox", MatLab. The routine minimizes the objective function, which is the H_2 -norm of the augmented system accounting for constraints on controller design parameters obtained from steering system performance and feel requirements.

Another important issue in the controller design is the balance between useful information transmitted to the driver from the road and unwanted disturbance and noise. This is achieved by proper selection of the bandwidth of the weighting function for the augmented plant in the optimal controller synthesis procedure.

R. McCann et al [17] investigated the robust stability of an electric power steering system in the conditions of high speed and wet road. In this situation, the characteristic equation of the linearized vehicle model has roots in the right-half complex plane. The

vehicle is stabilized by the use of yaw and lateral acceleration state feedback to electric power steering assist mechanism. The penalty is that the feedback increases damping and reduces the settling time in response to the steering transient.

The minimax control problem is the natural mathematical formulation to achieve the optimal performance of the control system under the requirements of robustness. The prominent example of the minimax method application is the H_∞ optimization. The performance measure that is minimized with H_∞ approach is the maximum value of the L_2 norm of system output over the class of exogenous signals that satisfy the L_2 norm bound. This elegant mathematical formulation can be too conservative in practice, because it does not take into account for information about spectrum of input signals. To accommodate this information the weighted functions (or filters) are usually used. But the question of the proper selection of the filters is beyond the scope of H_∞ theory. This drawback can be eliminated by considering more general minimax control problems. The importance of minimax optimization for the system with component-wise bounded inputs was highlighted in [19], where the measure of robust performance for such system was introduced. The LMI based solution for the minimax optimization problem with L_2 norm constraints on the components of input signal was proposed in [20].

The method of moment restraints (MMR) proposed in [21] and formulated in the general form in [22], solves the minimax control problem for the stationary exogenous input under arbitrary convex limitations on its spectrum. In MMR approach the assumptions are made that the class of inputs is defined by means of finite or number of integral (moment) restrictions on the special measure of signals. This approach includes as special cases both H_∞ and LQG optimal control.

For the problems with finite number of moment restrictions on the input spectrum the optimal control is constructed by reducing the minimax control problem to the problem of convex programming. From the practical standpoint, it is important to consider the separate limitations on the components of the exogenous input. Such limitations fall within the framework of MMR and can be accounted for by proposed general optimization procedure. In [23], the MMR approach was applied to the design of the active flywheel controller. However, it should be noted that the formulated convex

programming problem in [22] is rather complex for the numerical solution and, moreover, the complexity of the problem grows fast with the size of the system.

Paper [18] shows that in the case of component-wise moment restrictions on the input signal the minimax control problem can be reduced to the minimization of a linear functional over the set of solutions of some system of linear matrix inequalities. The latter problem is standard for the method of LMI [24]. It can be solved by efficient polynomial-time algorithm [25] that is realized in “LMI toolbox” [26]. The LMI reformulation of minimax control problem has one more benefit. It admits to combine the minimax optimization with pole placement constraints [27] and to consider multi-object optimization [28].

The EPS system has two inputs: one of which is the driver command and another is noise in the measurement of this command. The driver command is dominated by low frequency signals. The sensor measures the elastic deformation of the steering column, which is proportional to the driver steering torque. The measurement noise is dominated by high frequency signals. Summing up one can see that the EPS system has two input signals. The spectral properties of that are not known exactly, but satisfy some known constraints. Thus the EPS design problem can be formulated in terms of minimax control with component-wise restriction on the inputs. On the base of the proposed optimization method the EPS controller was constructed that satisfies the design objective in [18].

M. Kurishige and T. Kifuku designed a practical controller, which controls the current of a motor to generate assist torque based on the output of the torque sensor [29]. The assist torque is set so that it is nearly proportional to the sensor output. In the vicinity of 30Hz the control system may oscillate, causing a driver to feel unpleasant steering-wheel vibration. In general, drivers tend to prefer a low level of steering torque during static steering. Accordingly, the challenge is to suppress steering-wheel vibration while at the same time reducing steering torque. An effective way of suppressing steering-wheel vibration is to incorporate a control measure that applies damping at the frequency where oscillation occurs. To reduce the cost, EPS system does not have a motor-speed sensor. The motor speed has been estimated in the low frequency region below 5Hz, but it has been difficult to estimate the motor speed in the vicinity of an oscillation frequency of 30Hz. The problem is solved by using an observer [30] to estimate motor speed, and

developing a damping compensator, which provides compensation based on the estimated motor-speed signal. This has result in comfortable static steering performance free of steering-wheel vibration.

P. Hingwe et al designed a loop-shaping controller to control the power steering system in heavy vehicles [4]. The difference between the reference steering wheel angle and actual steering wheel angle is the input to the controller. The output of the controller is the torque command to the ECU. The controller is used to regulate the steering wheel position error to zero. The strategy is high gain at low frequency and to add phase lead selectively at the target gain cross over frequency. To avoid an excitation of high frequency dynamics, a roll off filter was added.

Another controller was designed by employing LQG technologies for a double pinion type EPS system [11]. The system is considered to be a two inputs and one output system. In the first case, the steering column torque is the input. In the second case, the motor angular position is the input. It is verified that, by the state-space model introduced in [11], the EPS system is controllable and observable. The locations of the closed loop poles that ensure required dynamics are obtained by a stochastic regulator. As the optimal feedback gain for the Linear Quadratic Regulator designed for a plant also minimizes the stochastic regulator cost function. And then, a Kalman filter is designed to obtain the required observer dynamics in the presence of stochastic disturbances. The LQR optimal controller by its nature ensures that the resulting closed loop system is asymptotically stable and has good robustness properties in terms of phase and gain margins [31].

A D-PI controller with a stabilization compensator is designed for an EPS product in Japan [32]. The D-PI controller controls the output of a motor aiding a steering operation in accordance with the value of a current control signal computed from a detected motor current and the value of a current command signal in accordance with a steering torque. A stabilization compensator is inserted into a later stage of a torque sensor for detecting a steering torque in order to improve the stability and responsiveness of the control system. The stabilization compensator has a function to eliminate a peak at a resonance frequency of resonance system including inertia and spring elements in the electric power steering system. The controller improves both the stability and response of a control system employed in an EPS system for vehicles by removing a peak value at the

resonance frequency and compensating for a phase shift at the phase frequency of a resonance system, which peak value and phase shift are included in a detected torque.

Another practical control solution from NSK Ltd., using two controllers, is claimed in [33]. The dual-microcontroller solution is also recommended by Motorola [34]. The control unit controls a motor for giving steering assist force to a steering mechanism, based on a current control value calculated from a steering assist command value and a current value of the motor. The steering assist command value is calculated based on the steering torque generated in the steering shaft. Based on a current command value calculated by the second controller, the second controller monitors the first controller that controls the driving of the motor based on the steering assist command value calculated by the first controller. When the first controller is in a status not controlling the steering assist command value, the function of the second controller for monitoring the first controller is limited.

1.3 MOTIVATION AND OBJECTIVE

The problem of the control design for an electric power steering system is considered as an example of the application of the developed technology. The purpose of the EPS system is to reduce the steering efforts of the driver by generating an assist torque. To this end, the torque produced by an assist motor has to be proportional with the given coefficient to the torque that is applied by the driver.

In an EPS system, the stability of the control system is sustained by means of a phase compensating circuit inserted into the later stage of a torque sensor. In addition, the response of the control apparatus deteriorates due to the moment of inertia of the motor joined to the steering system, worsening the feeling of steering operation. In addition, an EPS system constitutes a resonance system comprising the motor and a torsion bar as a mass and spring elements respectively. When the resonance system trigger the vibration, the feeling of steering operation worsens.

However, the stability and the response of the control system in an EPS system are antagonistic characteristics opposing each other. To be more specific, if the stability is improved, the responsiveness is deteriorated and, if the responsiveness is enhanced, on the other hand, the stability inevitably worsens. In other words, it is difficult to improve both of the characteristics at the same time. In addition, a band-eliminating filter is used

for eliminating a resonance frequency component generated by a resonance system comprising, among other components, the motor and the torsion bar included in the EPS system [32].

In addition, it is desirable to provide a nonlinear characteristic of system such as the hydraulic power steering system to the command specifying a steering power for aiding the manual steering operation. However, problems arise due to the fact that, in the case of hydraulic power steering system, it is difficult to design a control system by taking the nonlinear characteristic into consideration or by taking variations in dynamic characteristics caused by different operating state into consideration. On the top of that, once a control system is designed, it is also difficult to implement the designed control system into a digital circuit because of the increase of the order of the control system.

Motivated by these limitations, the objective of this thesis is to design a H_∞ robust controller for an EPS system, which takes into account environment disturbance and the requirements of the optimum steering feel. In order to achieve the desired performance and stability, a comprehensive and realistic model is derived first.

This model is derived from the physical characteristics of the components within an EPS system. In order to validate the proposed model, extensive simulations are performed in MatLab™ and CarSim™.

The second part of the thesis consists of designing a robust H_∞ controller for an EPS system. This controller design is based on the proposed dynamic model and derived by MatLab robust control Toolbox. Extensive simulations are carried out using MatLab™ and CarSim™ to demonstrate the performance, stability and robustness of the EPS system.

The third and final objective of this thesis is to prepare this controller for an experimental implementation on an available EPS system. With this scope, the proposed controller is described in implementation-ready algorithmic form. Future work will deal with the physical implementation of this algorithm and realization in an embedded DSP controller.

1.4 CONTRIBUTION

In this section, an outline of my research work will be presented.

1.4.1 EPS MODEL DERIVATION

In order to design a model-based controller, an EPS dynamic model was proposed. First, a real EPS system was divided into some mechanical or electronics components and then derived the dynamic model for each component. Finally, all the components were connected according to the real system architecture and the component-wise model can be derived. From a mechanical point of view, the steering system is made of, or modeled with, many masses or inertias lumped together with springs and dampers, or friction elements. Considering of the fact that high stiffness contributes to high frequency mode that usually are inconsequential to the fundamental behaviours of the system, which is dominated by low frequency mode, the model can be simplified by getting rid of some stiffness components. In this EPS model, the dynamic model of both of the mechanical parts, steering wheel and rack & pinion, are reduced because their stiffness is much higher than the stiffness of torque sensor.

1.4.2 NEW CONTROLLER ARCHITECTURE

To make it easier to design a control system, which can control the behavior of the system, new controller architecture was proposed. The traditional controller architecture, which is motor control plus compensator, has its own limitation because the controller is not sensitive to disturbance signal due to the position of the controller. As an alternative way, some extra sensors, such as yaw sensors or position sensors, can be added to send more information to the controller. Actually, the position of the controller has been changed logically with the extra sensors. In the proposed controller architecture, new controller is added without any extra peripherals. The advantage is that there is no cost penalty and the system reliability increased.

1.4.3 ROBUST CONTROL SYSTEM DESIGN

Based on the proposed controller architecture, a robust control system design can be divided into two stages: motor controller design and motion controller design.

A PI controller is designed to speed up the response of the electric motor. An electric motor is an over-damping system, so D-controller is not proper for motor control. Try-error technology is used and various coefficient combinations have been tested.

A H_{∞} controller is designed to attenuate the disturbance torque from the road wheel to the driver. One of the information received by the driver is the reaction torque,

corresponding to the input from the rack shaft, which is directly connected to the tires. A better road feel can be achieved by transmitting the information selectively. If the disturbance is modeled as high frequency bounded noise, the system with H_∞ controller is not sensitive to the disturbance signal, but sensitive to the necessary information from the road, which is the road feel. To compare with the traditional control system, H_∞ control system attenuates the noise and enhances the necessary information. As a result, this system has a better road feel.

If the disturbance is modeled as white noise, the simulation shows that the performance of H_∞ control system gets worse, and it is even worse than the traditional controller. The H_∞ control system is not suitable to attenuate the white noise.

1.5 THESIS OVERVIEW

The dissertation of this thesis is organized as follows. Chapter 2 contains the preliminary theory. Chapter 3 presents the derivation of the dynamic model for an EPS system. This chapter includes the modeling of the dynamics of each component, the derivation of the mechanical assembly and the reduction of the model. At the end of this chapter, the dynamic model is verified in MatLab™ and CarSim™. The new controller architecture is proposed in chapter 4, and in the same chapter, a robust EPS control system is designed based on the presented model and the controller architecture. Chapter 5 contains the detail of simulation and the discussion on the simulation results. Chapter 6 contains some conclusions and recommendation for future work.

On a final note on the text of this thesis, it is indicated that variables in **bold** format refer to matrix or vector quantities, whereas variables not in bold format refer to scalar quantities. Words in *italic* format refer to the MatLab routines. The use “*italic*” refer to a block name.

CHAPTER 2:PRELIMINARY THEORY

In this chapter, a short survey will be presented to introduce some technology of robust and optimum control. It starts with the introduction of the concept of vector norms and matrix norms. The next section gives a short survey of robust and optimum control theory. Finally, I will present the universal and MatLab solution of the H_∞ problem.

2.1 VECTOR NORMS AND MATRIX NORMS

The most important objective of a control system is to achieve certain performance specifications in addition to providing the internal stability. One way to describe the performance specifications of a control system is in terms of the size of certain signals of interest. So the concept of ‘norm’ is very important.

Let X be a vector space, a real-valued function $\|\cdot\|$ define on X is said to be a ‘norm’ on X if it satisfies the following properties:

- 1) $\|x\| \geq 0$ (positivity);
- 2) $\|x\| = 0$ if and only if $x = 0$ (positive definiteness);
- 3) $\|\alpha x\| = |\alpha| \|x\|$, for any scalar α (homogeneity);
- 4) $\|x + y\| \leq \|x\| + \|y\|$ (triangle inequality)

for any $x \in X$ and $y \in X$. A function is said to be a ‘semi-norm’ if it satisfies 1), 3) and 4) but not necessarily 2).

Let $x \in C^n$. Then we define the vector p -norm of x as

$$\|x\|_p := \left(\sum_{i=1}^n |x_i|^p \right)^{1/p}, \text{ for } 1 \leq p \leq \infty.$$

In particular, when $p = 1, 2, \infty$ we have

$$\|x\|_1 := \sum_{i=1}^n |x_i|;$$
$$\|x\|_2 := \sqrt{\sum_{i=1}^n |x_i|^2};$$

$$\|x\|_{\infty} := \max_{1 \leq i \leq n} |x_i|.$$

Clearly, norm is an abstraction and extension of our usual concept of length in 3-dimensional Euclidean space. So a norm of a vector is a measure of the vector “length”, for example $\|x\|_2$ is the Euclidean distance of the vector x from the origin. Similarly, we can introduce some kind of measure for a matrix.

Let $A = [a_{ij}] \in C^{m \times n}$, then the matrix norm induced by a vector p -norm is defined as

$$\|A\|_p := \sup_{x \neq 0} \frac{\|Ax\|_p}{\|x\|_p}$$

In particular, for $p = 1, 2, \infty$, the corresponding induced matrix norm can be computed as

$$\|A\|_1 = \max_{1 \leq j \leq n} \sum_{i=1}^m |a_{ij}| \quad (\text{column sum});$$

$$\|A\|_2 = \sqrt{\lambda_{\max}(A^* A)};$$

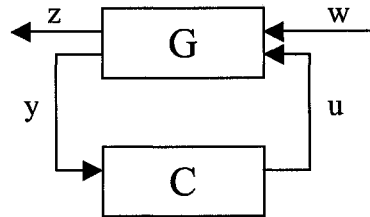
$$\|A\|_{\infty} = \max_{1 \leq i \leq m} \sum_{j=1}^n |a_{ij}| \quad (\text{row sum}).$$

The matrix norms induced by vector p -norms are sometimes called induced p -norms. This is because $\|A\|_p$ is defined by or induced from a vector p -norm. In fact, A can be viewed as a mapping from a vector space C^n equipped with a vector norm $\|\cdot\|_p$ to another vector space C^m equipped with a vector norm $\|\cdot\|_p$. So from a system theoretical point of view, the induced norms have the interpretation of input/output amplification gains.

2.2 ROBUST AND OPTIMAL CONTROL THEORY

The general area of methods for multivariable feedback design is well covered in the book [36], where the importance of frequency response interpretations is emphasized. One of the motivations for the original introduction of H_{∞} methods was to bring plant uncertainty, specified in the frequency domain, back into the centre-stage, as it had been in classical control in contrast to analytic methods such as LQG [37]. The H_{∞} norm was found to be appropriate for specifying both the level of plant uncertainty and the signal gain from disturbance inputs to error outputs in the controlled system.

The H_∞ optimal control problem is concerned with the following block diagram:



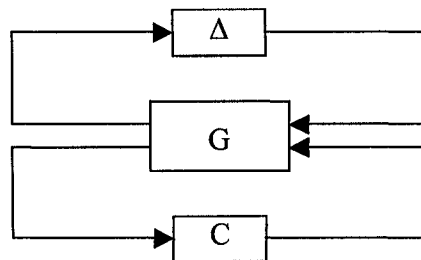
where

- w an external disturbance,
- y the measurement available to the controller,
- u the output from the controller,
- z an error signal that is desired to keep small,
- G the conventional plant to be controlled and any weighting functions included to specify the desired performance,
- C the controller to be designed.

The H_∞ optimal control problem is to design a stabilizing controller, C, so as to minimize the closed loop transfer function from w to z, T_{zw} , in the H_∞ norm, where

$$\|T_{zw}\|_\infty = \sup_w \bar{\sigma}(T_{zw}(j\omega))$$

The H_∞ norm gives the maximum energy gain, or sinusoidal gain of the system. This is in contrast to the H_2 norm, $\|T_{zw}\|_2$, which for example gives the variance of the output given white noise disturbances. The important property of the H_∞ norm comes from the application of the small gain theorem, which states that if $\|T_{zw}\|_\infty \leq \gamma$, then the system with block diagram,



will be stable for all stable Δ with $\|\Delta\|_\infty < 1/\gamma$. It is probably the case that this robust stability consequence was the main motivation for the development of H_∞ methods rather than the worst-case signal gain.

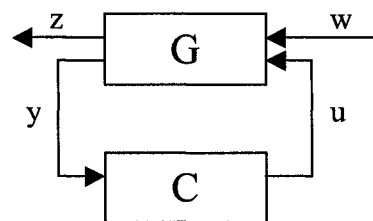
The first solution to a general rational MIMO H_∞ optimal control problem presented in [38]. The solution relied heavily on state-space methods. The procedure involved state-space inner/outer and coprime factorizations of transfer function matrices, which reduced the problem to a Nehari/Hankel norm problem solvable by the state-space method [39].

The simple state space H_∞ controller formulae were first announced by Glover and Doyle [40]. Independent encouragement for a simpler approach to the H_∞ problem came from papers [41,42]. They showed that the state-feedback H_∞ problem can be solved by solving an algebraic Riccati equation and completing the square. The state-space theory of H_∞ has been carried much further, by generalizing time-invariant to time-varying, infinite horizon to finite horizon, and finite dimensional to infinite dimensional and even to some nonlinear results. Some of these developments also provided alternative derivations of the standard H_∞ results.

Having established that the above H_∞ control problem can be relatively easily solved and can represent specifications for performance and robustness, let us return to the question of whether this gives a suitable robust control design tool. There is no question that the algorithm can be used to provide poor controllers due to poorly chosen problem descriptions resulting in, for example, very high bandwidth controllers.

2.3 H_∞ CONTROLLER DESIGN

In this section, some results from H_∞ control design are given based on the research in [35]. Consider the control system shown below:



The system equations are as follows:

$$\dot{x} = Ax + B_1 w + B_2 u$$

$$z = C_1 x + D_{11} w + D_{12} u$$

$$y = C_2 x + D_{21} w + D_{22} u$$

where $x \in R^n, y \in R^p, z \in R^{q_1}$, and $w \in R^n$ is a disturbance signal. Let T_{zw} be the closed-loop matrix transfer function from w to z . H_∞ control problem is to find a control law

$$u = K(s)y$$

such that the closed-loop system is stable and

$$\|T_{zw}\|_\infty < \gamma, \text{ where } \|T_{zw}\|_\infty = \sup_w \bar{\sigma}\{T_{zw}(jw)\}$$

for some pre-specified $\gamma > 0$.

2.3.1 STATE FEEDBACK DESIGN

For state feedback design, the following assumptions are made:

- 1) (A, B_2) is stabilizable,
- 2) $R_1 := D_{12}^T D_{12} > 0$,
- 3) $\begin{bmatrix} A - jwI & B_2 \\ C_1 & D_{12} \end{bmatrix}$ has full column rank for all w .

There exists a state feedback controller such that $\|T_{zw}\|_\infty < \gamma$ if and only if there is a stabilizing solution $X_\infty \geq 0$ solving

$$A_x^T X_\infty + X_\infty A_x + X_\infty (B_1 B_1^T / \gamma^2 - B_2 R_1^{-1} B_2^T) X_\infty + Q = 0,$$

where $A_x := A - B_2 R_1^{-1} D_{12}^T C_1$ and $Q := C_1^T (I - D_{12} R_1^{-1} D_{12}^T) C_1$.

2.3.2 OUTPUT FEEDBACK DESIGN

We shall make the following standard assumptions:

- 1) (A, B_2) is stabilizable and (C_2, A) is detectable,
- 2) $R_1 := D_{12}^T D_{12} > 0, R_2 := D_{21} D_{21}^T > 0$,
- 3) $\begin{bmatrix} A - jwI & B_2 \\ C_1 & D_{12} \end{bmatrix}$ has full column rank for all w ,
- 4) $\begin{bmatrix} A - jwI & B_1 \\ C_2 & D_{21} \end{bmatrix}$ has full row rank for all w .
- 5) $D_{12}^T C_1 = 0$ and $B_1 D_{21}^T = 0$.

So $A_x = A$ and $Q = C_1^T C_1$.

Clearly, state feedback design should have a solution if we want to consider the output feedback design. Hence, there exists a stabilizing solution $X_\infty \geq 0$ for:

$$A^T X_\infty + X_\infty A + X_\infty (B_1 B_1^T / \gamma^2 - B_2 R_1^{-1} B_2^T) X_\infty + C_1^T C_1 = 0$$

and H_∞ state feedback gain becomes $F_\infty = -R_1^{-1} B_2^T X_\infty$. It is well known that there may exist many H_∞ output feedback controllers.

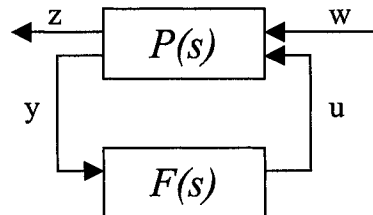
2.3.3 H_∞ SYNTHESIS USING MATLAB™

The methods of H_∞ synthesis are especially powerful tools for designing robust multivariable feedback control systems to achieve singular value loop shaping specification, as presented in [45]. The Robust Control Toolbox functions *hinfn* and *hinfnpt* compute continuous-time H_∞ control law; their discrete-time counterparts are *dhinfn* and *dhinfnpt*. The H_∞ design problem can be formulated as follows.

Given a state-space realization of an “augmented plant” $P(s)$

$$P(s) := \begin{bmatrix} A & B_1 & B_2 \\ C_1 & D_{11} & D_{12} \\ C_2 & D_{21} & D_{22} \end{bmatrix}$$

as in the following diagram



find a stabilizing feedback control law

$$u(s) = F(s)y(s)$$

such that the norm of the closed-loop transfer function matrix

$$T_{zw} = P_{11}(s) + P_{12}(s)(I - F(s)P_{22}(s))^{-1}F(s)P_{21}(s)$$

is small. Two such problems addressed by the Robust Control Toolbox are

$$H_\infty \text{ Optimal Control: } \min \|T_{zw}\|_\infty$$

$$\text{Standard } H_\infty \text{ control: } \|T_{zw}\|_\infty < 1$$

The standard H_∞ control is sometimes also called the H_∞ small gain problem. The entire design procedure is simple and requires only “one parameter” γ -iteration of the following flow-chart, as shown in Figure 2-1.

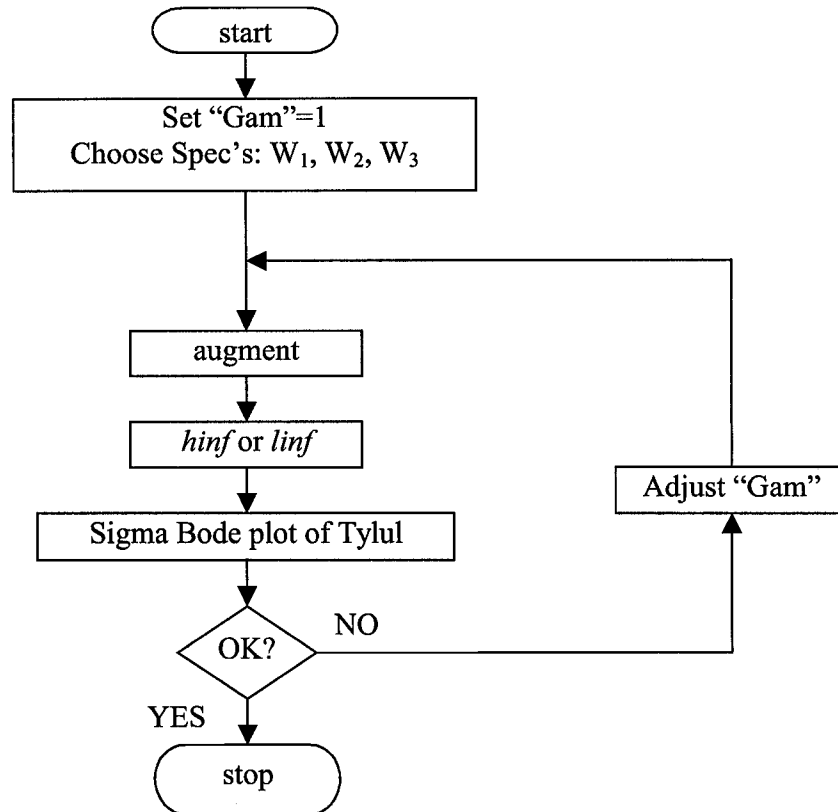


Figure 2-1: H_∞ synthesis using MatLab

The H_∞ theory gives four conditions for the existence of a solution to the standard H_∞ control problem:

1. D_{11} small enough. There must exist a constant feedback control law

$$F(s) = \text{“constant matrix”}$$

Such that the closed-loop D matrix satisfies

$$\bar{\sigma}(D) < 1$$

2. Control Riccati $P \geq 0$. The H_∞ full-state feedback control Riccati equation must have a real, positive semidefinite solution P . The software ascertains existence of the Riccati solution by checking that the associated Hamiltonian matrix does not have any $j\omega$ -axis eigenvalues. Positive semidefiniteness of the solution is verified by checking, equivalently, that the H_∞ full-state feedback control law is

asymptotically stabilizing [46]; this circumvents numerical instabilities inherent in directly checking positive semidefiniteness.

3. Observer Riccati $S \geq 0$. The Riccati equation associated with the observer dual of the H_∞ full-state feedback control problem must have a real, positive semidefinited solution S . Again the results of [46] are used to avoid numerical instabilities.
4. $\lambda(PS) < 1$. The greatest eigenvalue of the product of the two Riccati equation solutions must be less than one.

All of these four conditions must hold for there to exist a feedback control law, which solves the standard H_∞ control problem. The functions *hinf* and *hinfot* automatically check each of these four conditions and produce displays indicating which, if any, of the conditions fail.

2.3.4 PLANT AUGMENTATION

The state-space or transfer function plant is augmented using functions *augss* and *augtf*.

Augss computes a state-space model of an augmented plant $P(s)$ with weighting functions $W_1(s)$, $W_2(s)$, and $W_3(s)$ penalizing the error signal, control signal and output signal respectively, as shown in Figure 2-2.

The close-loop transfer function matrix is the weighted mixed sensitivity

$$T_{y,u_1} \triangleq \begin{bmatrix} W_1 S \\ W_2 F S \\ W_3 T \end{bmatrix}$$

where S and T are the sensitivity and complementary sensitivity matrices

$$S = (I + GF)^{-1}$$

$$T = GF(I + GF)^{-1}$$

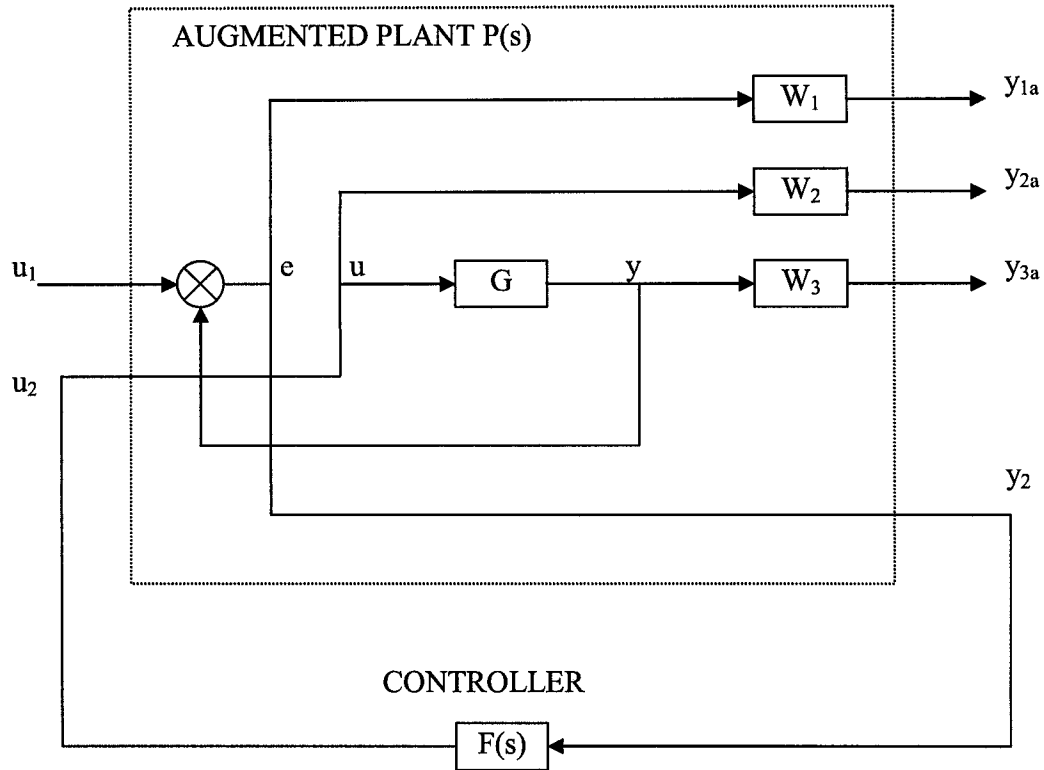


Figure 2-2: Plant Augmentation

The transfer functions $G(s)$, $W_1(s)$ and $W_2(s)G(s)$ must be proper, i.e., bounded as $s \rightarrow \infty$. However, $W_3(s)$ may be improper. Input data of *augss* are the state-space matrices of $G(s)$, $W_1(s)$ and $W_2(s)G(s)$. The augmented plant $P(s)$ produced by *augss* is

$$P(s) = \begin{bmatrix} W_1 & -W_1G \\ 0 & W_2 \\ 0 & W_3G \\ I & -G \end{bmatrix}$$

with state-space realization

$$P(s) := \begin{bmatrix} A & B_1 & B_2 \\ C_1 & D_{11} & D_{12} \\ C_2 & D_{21} & D_{22} \end{bmatrix} = \begin{bmatrix} A_G & 0 & 0 & 0 & 0 & B_G \\ -B_{W_1}C_G & A_{W_1} & 0 & 0 & B_{W_1} & -B_{W_1}D_G \\ 0 & 0 & A_{W_2} & 0 & 0 & B_{W_2} \\ B_{W_3}C_G & 0 & 0 & A_{W_3} & 0 & B_{W_3}D_G \\ -D_{W_1}C_G & C_{W_1} & 0 & 0 & D_{W_1} & -D_{W_1}D_G \\ 0 & 0 & C_{W_2} & 0 & 0 & D_{W_2} \\ \tilde{C}_G + D_{W_3}C_G & 0 & 0 & C_{W_3} & 0 & \tilde{D}_G + D_{W_3}D_G \\ -C_G & 0 & 0 & 0 & I & -D_G \end{bmatrix}$$

where

$$\begin{aligned} \tilde{C}_G &= P_0C_G + P_1C_GA_G + \dots + P_nC_GA_G^{n-1} \\ \tilde{D}_G &= P_0D_G + P_1C_GB_G + \dots + P_nC_GA_G^{n-2}B_G \end{aligned}$$

augtf calls *augss* internally after a series of transfer function to state-space transformations on W_1 , W_2 , and W_3 .

Note that if the augmented plant is to be used for H_∞ synthesis via *hinf* or *linf*, then it is essential that the weights W_1 , W_2 and W_3 be selected so that the augmented plant has a “ D_{12} ” matrix of full column rank. An easy way to ensure that this is the case is to choose a $W_2(s)$ with an invertible “ D -matrix”, e.g., $W_2(s) = \varepsilon I$ where ε is any non-zero number.

2.4 SINGULAR-VALUE LOOP SHAPING

Consider the multivariable feedback control system shown in Figure 2-3, as presented in [35].

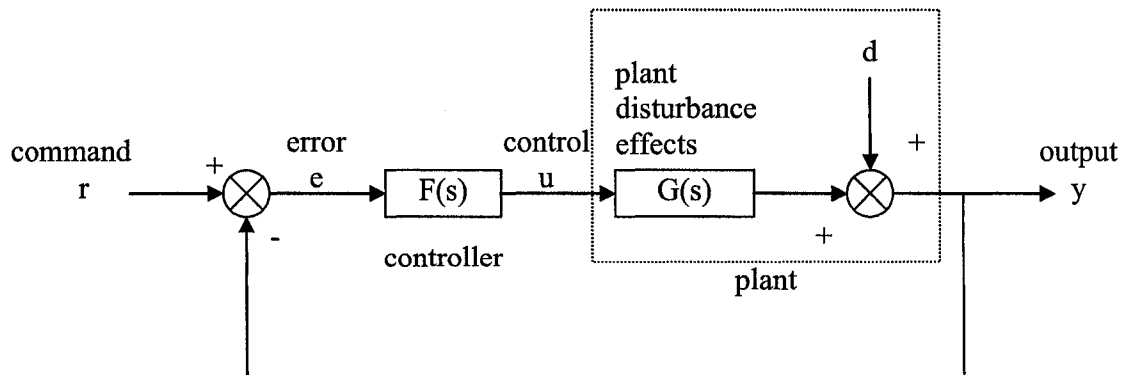


Figure 2-3: Traditional Feedback Control System

In order to quantify the multivariable stability margins and performance of such systems, one can use the singular values of the closed-loop transfer function matrices from r to each of the three outputs e , u and y .

$$\begin{aligned} S(s) &\stackrel{def}{=} (I + L(s))^{-1} \\ R(s) &\stackrel{def}{=} F(s)(I + L(s))^{-1} \\ T(s) &\stackrel{def}{=} L(s)(I + L(s))^{-1} = I - S(s) \end{aligned}$$

where $L(s) = G(s)F(s)$.

The two matrices $S(s)$ and $T(s)$ are known as the **sensitivity function** and **complementary sensitivity function**, respectively. The matrix $R(s)$ has no common name. The singular value Bode plot of each of the three transfer function matrices S , R , and T play an important role in robust multivariable control system design. The singular values of the loop transfer function matrix $L(s)$ are important because L determines the matrices $S(s)$ and $T(s)$.

The singular values of S determine the disturbance attenuation since S is in fact the closed-loop transfer function from disturbance d to plant output y . Thus a disturbance attenuation performance specification may be written as

$$\bar{\sigma}(S(j\omega)) \leq |W_1^{-1}(j\omega)|$$

where $|W_1^{-1}(j\omega)|$ is the desired disturbance attenuation factor. Allowing $W_1(j\omega)$ to depend on frequency ω enables the designer to specify a different attenuation factor for each frequency ω .

The singular value Bode plots of $R(s)$ and of $T(s)$ are used to measure the stability margins of multivariable feedback designs in the face of additive plant perturbations (Δ_A) and multiplicative plant perturbations (Δ_M), respectively.

Let us consider how the singular value bode plot of complementary sensitivity $T(s)$ determines the stability margin for multiplicative perturbations Δ_M . The multiplicative stability margin is, by definition, the “size” of the smallest stable $\Delta_M(s)$ which destabilizes the system in Figure 2-4 with $\Delta_A = 0$.

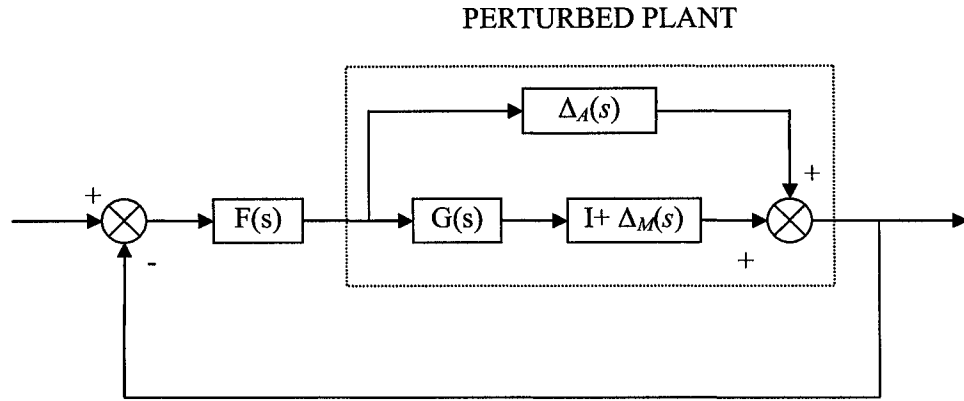


Figure 2-4: Additive/Multiplicative uncertainty.

Taking $\bar{\sigma}(\Delta_M(j\omega))$ to be the definition of the “size” of $\Delta_M(j\omega)$, the following stability theorem can be concluded:

Robustness Theorem 1: Suppose the system in Figure 3-2 is stable with both Δ_A and Δ_M being zero. Let $\Delta_A = 0$. Then the size of the smallest stable Δ_M for which the system becomes unstable is

$$\bar{\sigma}(\Delta_M(j\omega)) = \frac{1}{\bar{\sigma}(T(j\omega))}$$

Robustness Theorem 2: Suppose the system in Figure 3-2 is stable with both Δ_A and Δ_M being zero. Let $\Delta_M = 0$. Then the size of the smallest stable Δ_A for which the system becomes unstable is

$$\bar{\sigma}(\Delta_A(j\omega)) = \frac{1}{\bar{\sigma}(R(j\omega))}$$

As a consequence of Theorems 1 and 2, it is common to specify the stability margins of control systems via singular value inequalities such as

$$\bar{\sigma}(R(j\omega)) \leq |W_2^{-1}(j\omega)|$$

$$\bar{\sigma}(T(j\omega)) \leq |W_3^{-1}(j\omega)|$$

where $|W_2(j\omega)|$ and $|W_3(j\omega)|$ are the respective sizes of the largest anticipated additive and multiplicative plant perturbations.

An important point to note in choosing design specifications W_1 and W_3 is that the 0 db crossover frequency the Bode plot of W_1 must be sufficiently below the 0 db crossover frequency of W_3^{-1} . More precisely, the following relationship is required

$$\bar{\sigma}(W_1^{-1}(j\omega)) + \bar{\sigma}(W_3^{-1}(j\omega)) > 1 \quad \forall \omega$$

CHAPTER 3:EPS DYNAMIC MODEL

3.1 INTRODUCTION

Generally, there are three types of EPS systems: column-type, rack-type and pinion-type, as shown in Figure 3-1. The selection of different configurations depends on the package and in-vehicle environment.

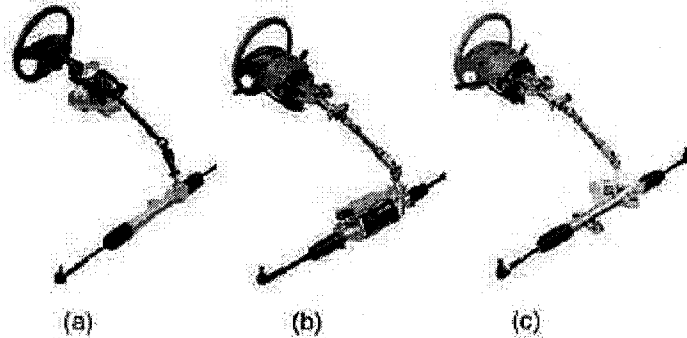


Figure 3-1: Three Types of Integrated Systems

(a): column-type, (b): rack-type, (c): pinion-type

This chapter is organized as follows. Section 3.2 contains the general description of a column-type EPS system. The dynamic model of each component is derived next, in section 3.3. Section 3.4 shows the dynamic model of the whole system. The verification of the dynamic model is given in section 3.5. Section 3.6 contains the state-space model and the analysis of disturbance and performance. The conclusions are in section 3.7.

3.2 THE GENERAL DESCRIPTION OF AN EPS SYSTEM

The schematic arrangement of a column-type EPS system is shown in figure 3-2.

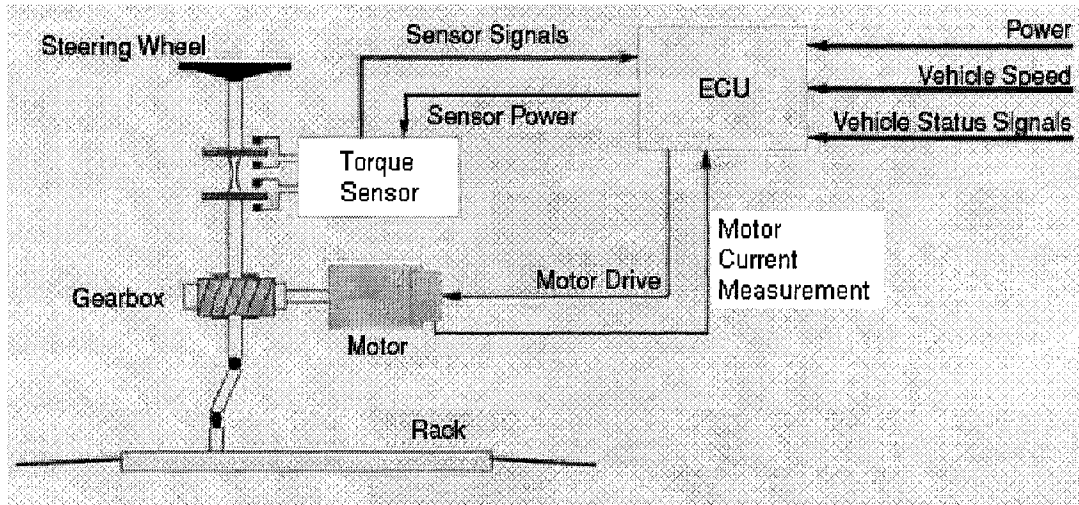


Figure 3-2: EPS Schematic Arrangement.

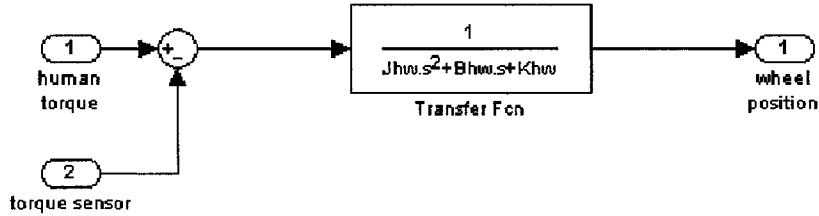
The EPS consists of a torque sensor, which senses the driver's movements of the steering wheel as well as the movements of the vehicle; an ECU, which performs calculations on assisting force based on signals from the torque sensor; a motor, which produces turning force according to the output from ECU; and a reduction gear, which increases the turning force from the motor and transfers it to the steering mechanism. The rest of the steering system: Steering Wheel (or hand wheel, HW), Intermediate Shaft (I-Shaft), and Rack & Pinion are also shown. Basically, the control procedure can be summarized as follows:

- 1) The torque sensor estimates the torque, which is the command from the human to steer the car, by the torsion bar mechanism inside.
- 2) ECU calculates the assistant torque based on the command torque (from torque sensor), the vehicle speed (from speed sensor or in-vehicle network) and the status of the electric motor, and then sends the command to the electric motor.
- 3) The electric motor generates the assistant torque according to the command from the ECU and transfers it to the column through a worm gear mechanism.
- 4) With the power assistance from the electric motor, the pinion and rack turns the wheels.

3.3 COMPONENT-WISE DYNAMIC MODEL

3.3.1 STEERING WHEEL DYNAMIC MODEL

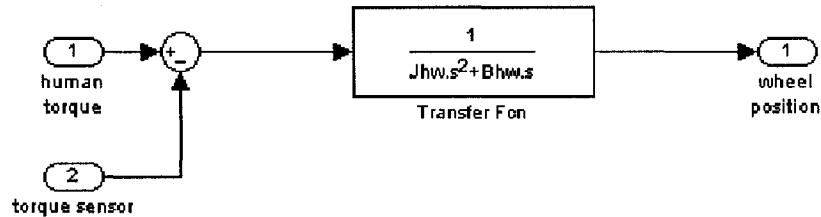
The upper part of the system model is the dynamic model of the human wheel. The MatLab model is as follows:



The differential equation of the steering wheel is:

$$T_h - T_s = J_{hw} \ddot{\theta}_{hw} + B_{hw} \dot{\theta}_{hw} + K_{hw} \theta_{hw} \quad (\text{Equ 1})$$

Where T_h and T_s are the torque from driver and torque sensor, respectively. θ_{hw} denotes the angle of rotation of the steering wheel. J_{hw} , B_{hw} and K_{hw} are moment of inertia, damping coefficient and stiffness coefficient. To simplify the model, the stiffness coefficient can be neglected. That is to say, the steering wheel is rigid connection. The dynamic model can be simplified as follows:

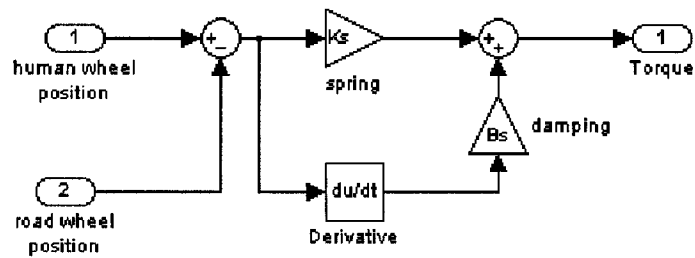


Using LapLace transform, the transfer function is:

$$\frac{\Theta_{hw}}{T_h - T_s} = \frac{1}{J_{hw}s^2 + B_{hw}s} \quad (\text{Equ 2})$$

3.3.2 TORQUE SENSOR DYNAMIC MODEL

The torque sensor is modeled as a torsion bar. The MatLab model is as follows:



The differential equation of the torque sensor is:

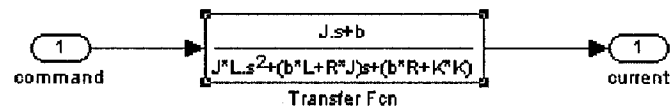
$$T_s = K_s (\theta_{hw} - \theta_{rw}) + B_s \frac{d(\theta_{hw} - \theta_{rw})}{dt} \quad (\text{Equ 3})$$

Where K_s , B_s denote the stiffness coefficient and damping rate of the torsion bar, respectively. θ_{rd} is the angle of rotation of the road wheel. Using Laplace transform, the transfer function is:

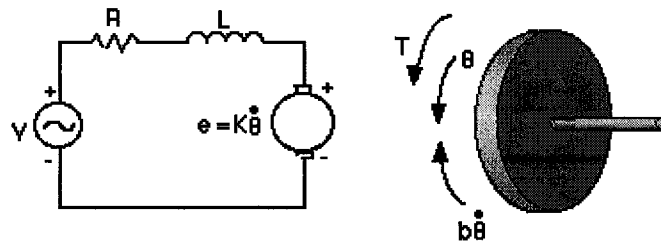
$$\frac{T_s}{\Theta_{hw} - \Theta_{rd}} = B_s \cdot s + K_s \quad (\text{Equ 4})$$

3.3.3 THE DYNAMIC MODEL OF A BRUSHED DC MOTOR

The model of the brushed DC motor is as follows:



A common actuator in an EPS system is the DC motor. It directly provides rotary motion and, coupled with wheels or drums and cables, can provide translational motion. The electric circuit of the armature and the free body diagram of the rotor are shown below.



Where

J	moment of inertia of the rotor
b	damping ratio of the mechanical system
K	electromotive force constant
R	electric resistance
L	electric inductance

From the figure above, the following equations (Equ 5) can be derived based on Newton's law combined with Kirchhoff's law:

$$\begin{aligned}
 J\ddot{\theta} + b\dot{\theta} &= Ki \\
 L\frac{di}{dt} + Ri &= v - K\dot{\theta}
 \end{aligned}
 \tag{Equ 5}$$

From the above modeling equations, the transfer function can be summarized using Laplace Transforms as Equ 6:

$$\begin{aligned}
 s(Js + b)\Theta(s) &= KI(s) \\
 (Ls + R)I(s) &= V - Ks\Theta(s)
 \end{aligned}
 \tag{Equ 6}$$

By eliminating θ , the following open-loop transfer function can be derived, as Equ 7:

$$\frac{I}{V} = \frac{Js + b}{(Js + b)(Ls + R) + K^2}
 \tag{Equ 7}$$

The motor torque, T , is proportional to the armature current, I , by a constant K_t . The open-loop transfer function is shown in Equ 8, where the torque is the output and the voltage is the input.

$$\frac{T}{V} = \frac{K(Js + b)}{(Js + b)(Ls + R) + K^2}
 \tag{Equ 8}$$

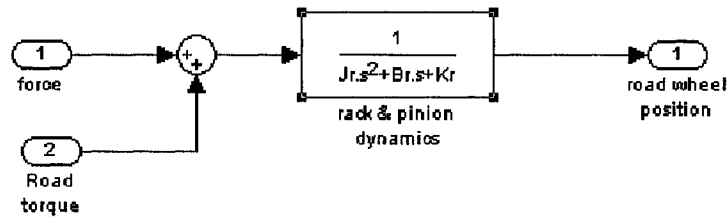
3.3.4 THE DYNAMIC MODEL OF PINION AND RACK ASSEMBLY

The pinion and rack is modeled as a mechanic system consists of a mass and a spring. The differential equation of the steering wheel is:

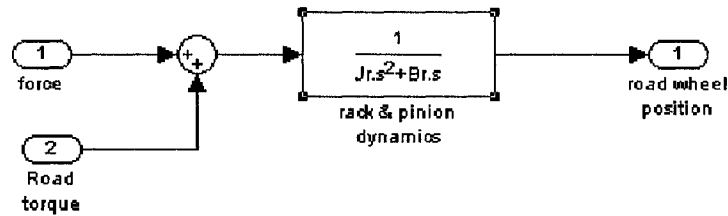
$$T_r + T_f = J_r\ddot{\theta} + B_r\dot{\theta} + K_r\theta
 \tag{Equ 9}$$

Where J_r , B_r and K_r are the moment of inertia, damping coefficient and stiffness coefficient, respectively. T_r and T_f denote torque from road wheels and steering torque, respectively. θ represents the road wheel position.

The model of the pinion and the rack is as follows:



Both of the force torque and the road torque have the same positive direction. Also to simplify the system, the stiffness coefficient is assumed to be zero. As a result, the model can be simplified as follows:



3.4 THE DYNAMIC MODEL OF AN EPS SYSTEM

The EPS system is modeled as a multi-input, multi-output (MIMO) system. The inputs and outputs are summarized below:

The inputs of the system are:

- 1) The command from the driver, which is the torque from the human hands to the steering wheel, measured in Nm.
- 2) The disturbance from the road, which is the torque from the road wheels to the rack and pinion mechanism, measured in Nm.

The outputs of the system are:

- 1) The steering wheel position, which is the steering angle, measured in degree.
- 2) The road feel to the driver, which is the reaction torque to the driver or the torque sensor output, measured in Nm.
- 3) The road wheel position, which is the angle of the road wheel, measured in degree.

In addition to the components described in section 3.3, an EPS system has other mechanical connections, which can be assumed as rigid connection, such as deduction gear. The deduction gear is modeled as a gain with the ratio of 20. The torque from the torsion bar and the torque transmitted through the deduction gear from the assist motor

are added up to supply the turning force to the pinion. The dynamic model of an EPS system is shown in Figure 3-3:

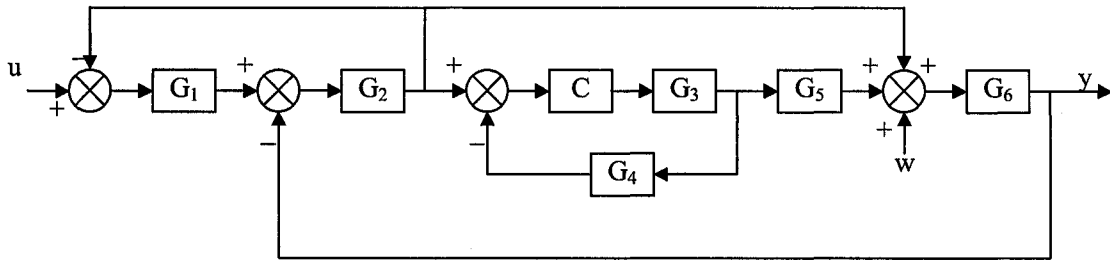


Figure 3-3: Presented EPS Dynamic Model

In the figure, the following nomenclature is used:

- G_1 : the dynamic model of hand wheel
- G_2 : the dynamic model of torque sensor
- C : the motor controller
- G_3 : the dynamic model of an electric motor
- G_4 : the current sensor
- G_5 : the dynamic model of reduction gear
- G_6 : the dynamic model of rack and pinion
- u : the torque from the driver
- w : the torque from the road
- y : the angle of the front road wheels

3.5 MODEL VERIFICATION

Simulations are required to compare the study-case EPS model with the commercial model in CarSim™. The verification is necessary because the dynamic model is the basis of the controller configuration.

Section 3.5.1 discusses the system stability. In section 3.5.2, a short description of CarSim is presented to show the reason why CarSim is employed as the virtual vehicle module in the simulation. The simulations are described in section 3.5.3. Comparisons between the proposed dynamic model and the commercial model are presented in section 3.5.4. Section 3.5.5 contains the conclusion and discussions.

3.5.1 SYSTEM STABILITY ANALYSIS

The system state matrix can be derived as follows:

$$\mathbf{A} = \begin{bmatrix} 0 & 1 & 0 & 0 & 0 & 0 \\ -151.5 & -0.7 & 0 & 0 & 151.5 & 0.0947 \\ 0 & 0 & 0 & 1 & 0 & 0 \\ 0 & 0 & -38 & -12 & 0 & 0 \\ 0 & 0 & 0 & 0 & 0 & 1 \\ 2597.4 & 1.623 & 3896.1 & 11688.3 & -2597.4 & 17.86 \end{bmatrix}$$

the eigenvector of the state matrix can be derived as:

$$eig = \begin{bmatrix} -8.5418 + 51.606i \\ -8.5418 - 51.606i \\ -1.4743 \\ -4.8412 \times 10^{-16} \\ -6 + 1.4142i \\ -6 - 1.4142i \end{bmatrix}$$

all the eigenvalues are in the left-half complex plane, so the system is stable.

3.5.2 VIRTUAL VEHICLE MODULE

The best way to verify the research result is to implement it in a real vehicle. An alternative way is to do simulation in software. In this way, simulated tests can be run far more quickly and easily. In this thesis, CarSim is used to stimulate the real vehicle dynamics. CarSim is mainly intended to simulate cars and light trucks. It shows how vehicles respond dynamically to inputs from the driver and the immediate environment [44]. It produces the same kinds of outputs that might be measured with physical tests involving instrumented vehicles.

Here are some reasons that CarSim makes simulation practical [44]:

1. It is much easier to use than older vehicle simulation program,
2. It requires no special hardware,
3. It runs fast,
4. The CarSim database minimizes the time needed to build a vehicle description and set up run conditions,
5. CarSim can provide accurate simulation results,

6. CarSim is designed to also work with MatLab/Simulink, so new controller and alternative component models can be added optionally.

3.5.3 SIMULATION DESCRIPTION

The EPS model is simulated using MatLab™, and the vehicle dynamics are simulated using CarSim™. The input/output signals of each module are listed in the table below.

Table 3-1: the input/output signals of each module

module	Input signals	Output singles
CarSim	the steering wheel angle	the front right wheel angle
		the front left wheel angle
		the vehicle speed
		the torque on the front right wheel
		the torque on the front left wheel
		the torque from the rack and pinion to the steering shaft
EPS	the torque to the rack and pinion from road wheels	The steering wheel angle
	Torque from the driver to the steering wheel	The road wheel angle
	The motor command	The torque signal from the torque sensor
	The motor current	The motor current
controller	The motor current	The motor command
	Torque signal from torque sensor	

The target vehicle used in the simulation is a built-in car model of CarSim™, named “Big Car: FWD Simulink ABS”. The configuration of the car is listed in the table 3-2.

The road selected in the simulation is one of the built-in road models in CarSim™. It is a straight, flat road with the rolling resistance of 1.0, which implies that the surface of the road is smooth concrete.

The external input of the simulation is the torque from the driver to the steering wheel, which is a pulse signal. The pulse amplitude is 1 and the pulse period is 5 seconds.

The pulse signal simulates the driver's manoeuvre of turning the wheel for 5 seconds and then releasing the wheel. The CarSim module acts as a duplicate steering system feedback the torque from road wheel to the steering shaft, which is complicated to model, according to the turning of the steering wheel. The output signals from both of the CarSim module and proposed EPS model will be compared to verify the proposed model.

Table 3-2: the configuration of the target vehicle

module	parts	configure
system	powertrain	2.5L, gear 4.4
	steering	Gear 16.0
	turning	No steering
	speed	Constant speed at 50Km/h
front	suspension	independent
	Left tire	205/60R14
	Right tire	205/60R14
rear	suspension	independent
	Left tire	205/60R14
	Right tire	205/60R14

3.5.4 SIMULATION RESULTS AND DISCUSSION

This section contains simulation results. By the time domain response comparison between the proposed dynamic model and the commercial model of CarSim™, the simulation results will be discussed. The Figure 3-4 to Figure 3-8 show the simulation results.

The testbench is built in MatLab/Simulink™. Figure 3-4 shows the diagram of the testbench and input pulse signal. Figure 3-5 shows the time domain response of the steering wheel under the driver's maneuvers. The reaction torque is the torque of the torque sensor. Figure 3-6 shows the comparison between the turning angles from CarSim model and the proposed model. In the proposed model, the turning angle of the front wheel, in fact, is the turning angle of the rack and pinion mechanical assembly of the front wheels. In a real vehicle, the two front wheels have a little angle difference with

each other and the angles are smaller than the turning angle of the rack, because of the existence of the small lag of angle between the two front wheels, which is called toe angle. The simulation result, shown in figure 3-6, illustrates that the curve from the CarSim model and the proposed model are almost identical. The curve of the CarSim model is a little smaller than that in the proposed model. Figure 3-7 shows the torque feedback from the front road wheels to the steering system, through the rack and pinion mechanical assembly. By the comparison between figure 3-5 and figure 3-7, the conclusion can be made that the reaction torque to the driver has similar curve, but inverse, with the torque from road wheels to the rack and pinion. One can conclude that, for the EPS system using PI controller, the driver have sufficient road feel, which is more than necessary. That is to say, the driver is feeling all the information from the road. Figure 3-8 shows that the vehicle speed does not change a lot during the steering maneuvers.

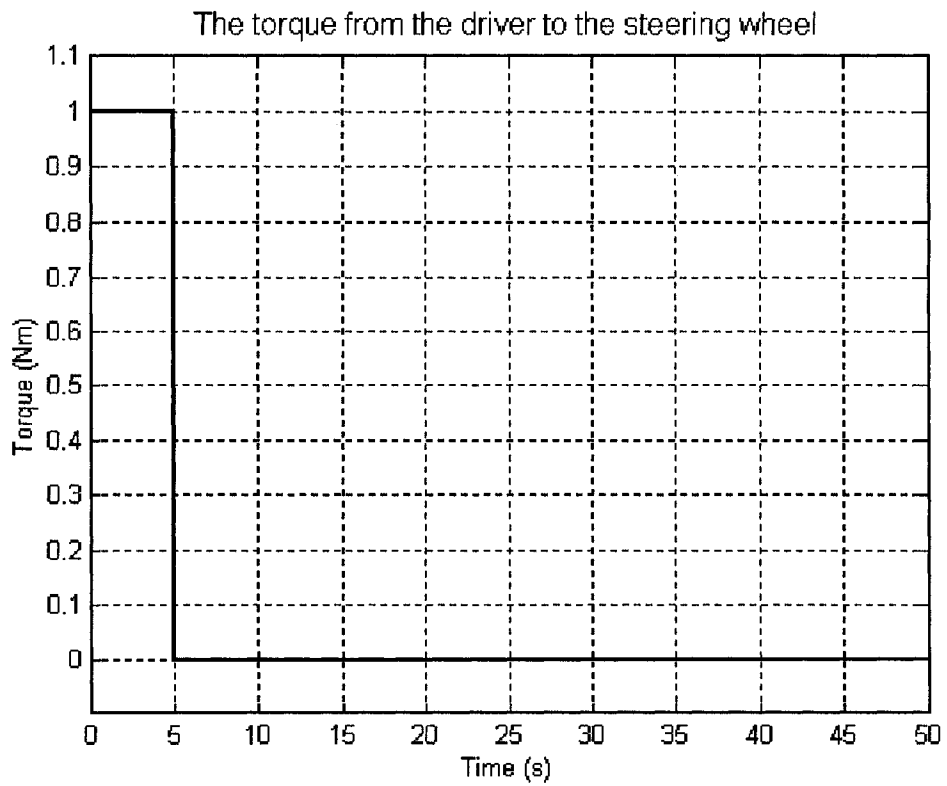
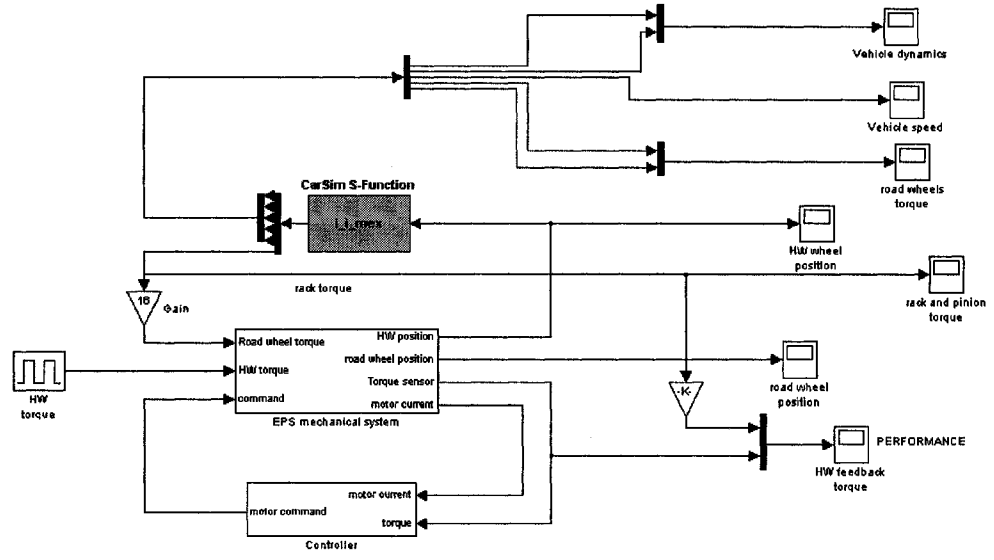


Figure 3-4: The Testbench and the System Input Signal

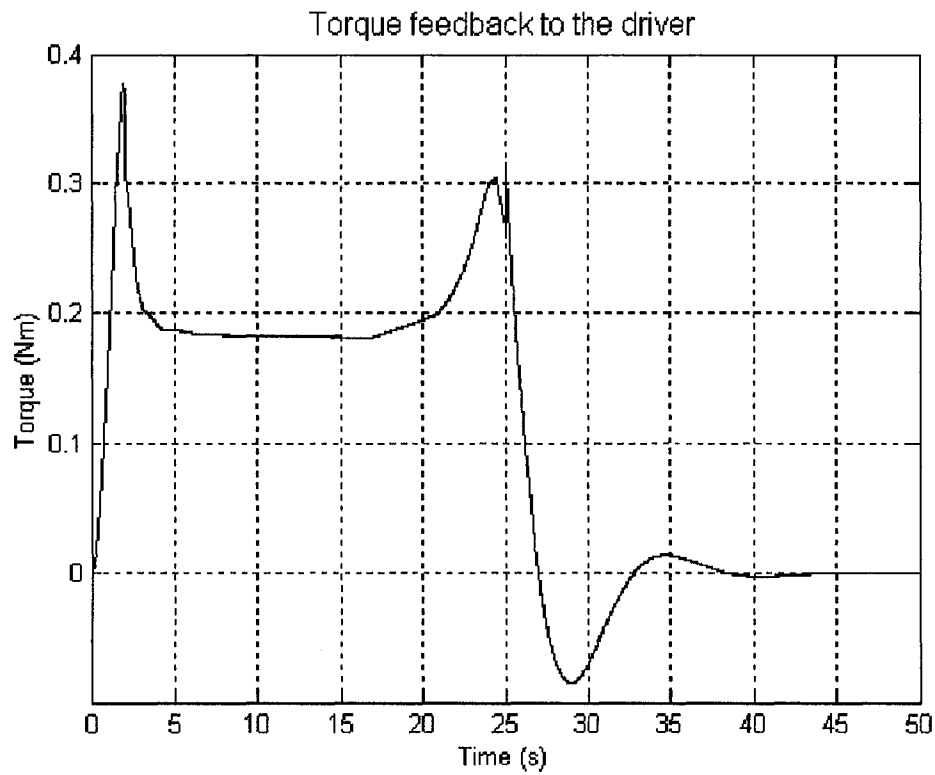
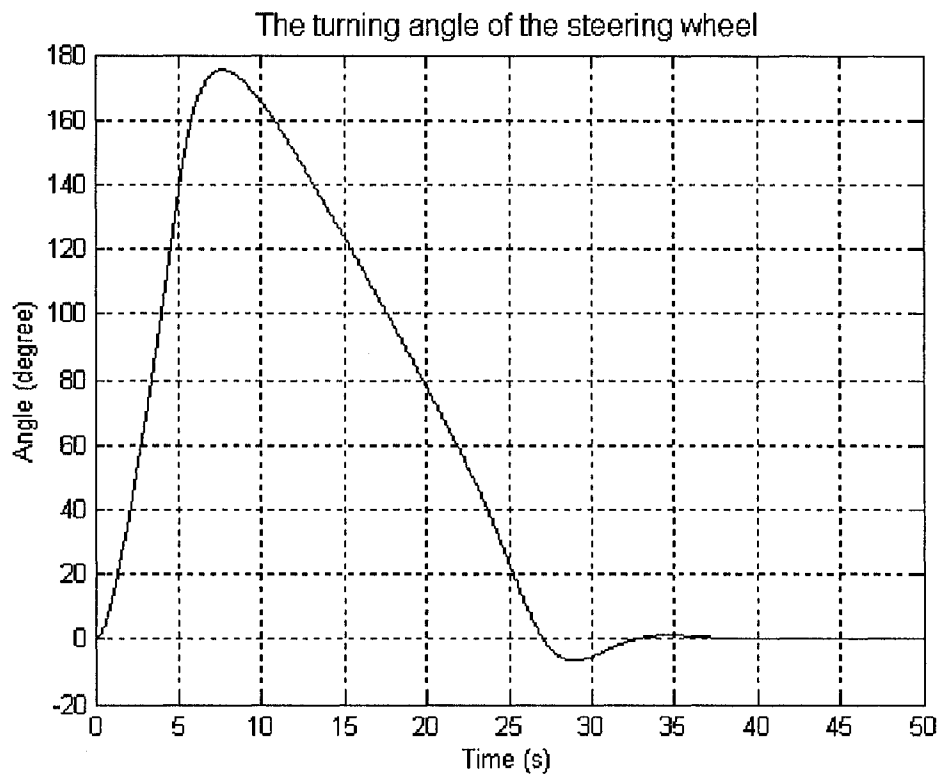


Figure 3-5: the Time Domain Response of the Steering Wheel

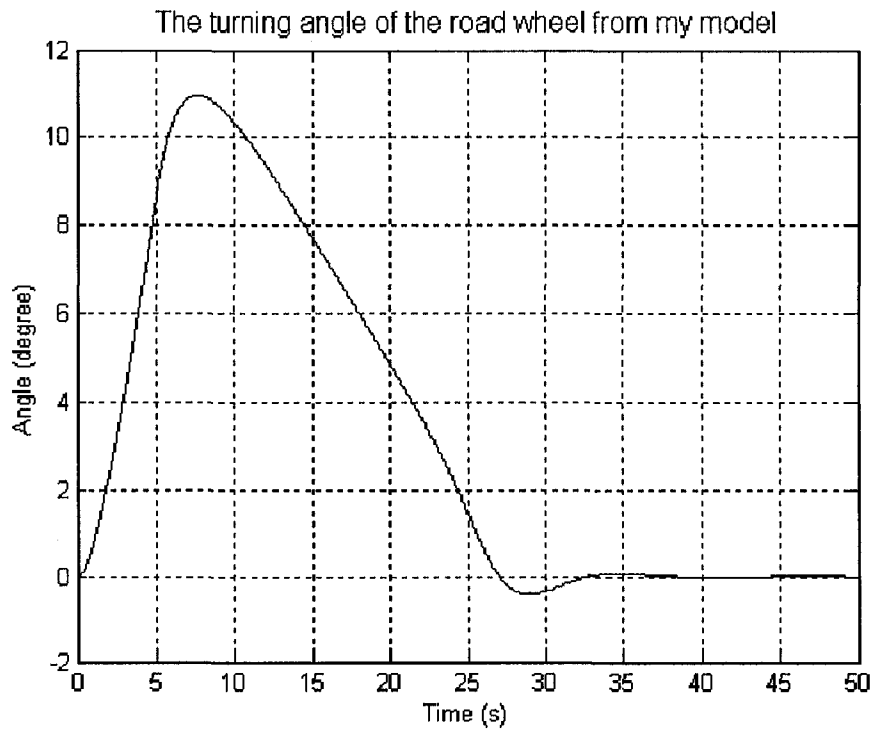
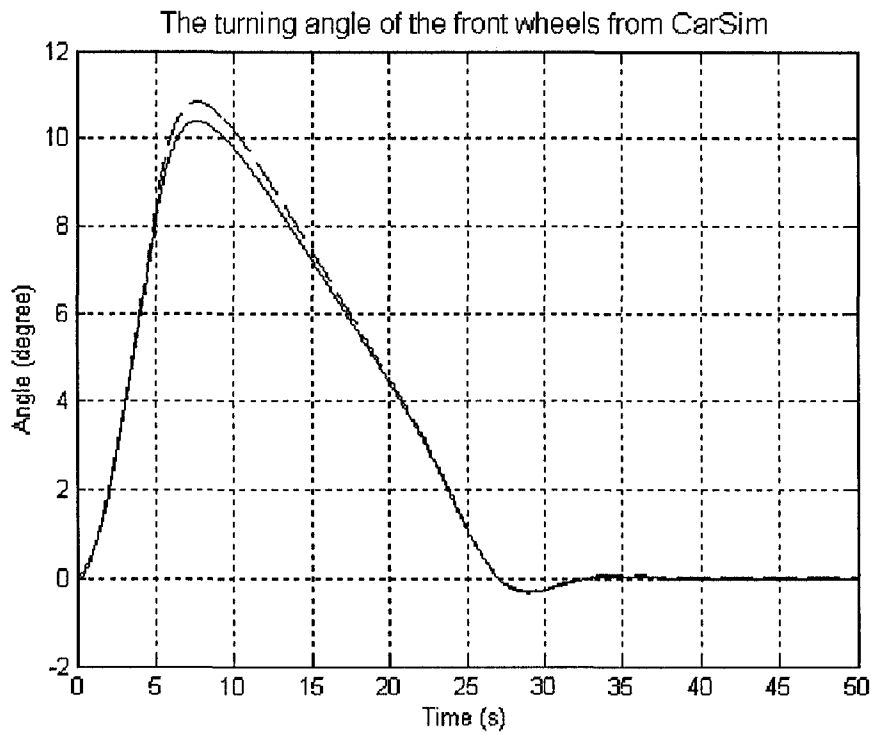


Figure 3-6: The Comparison Between the Angles of the Front Road Wheels from CarSim and the Presented Model

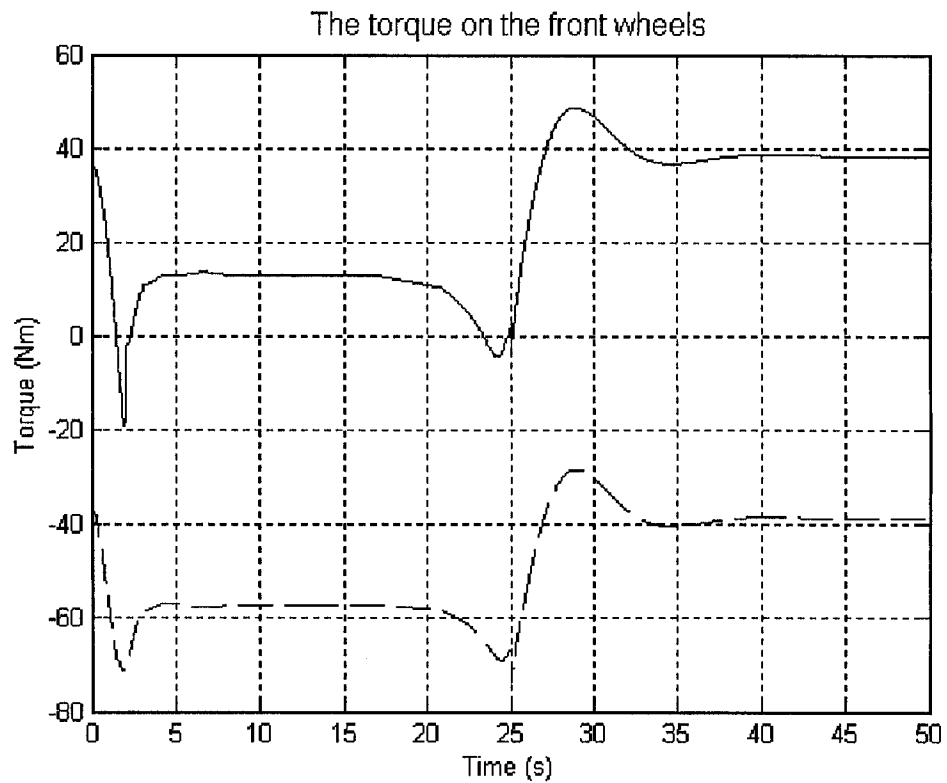
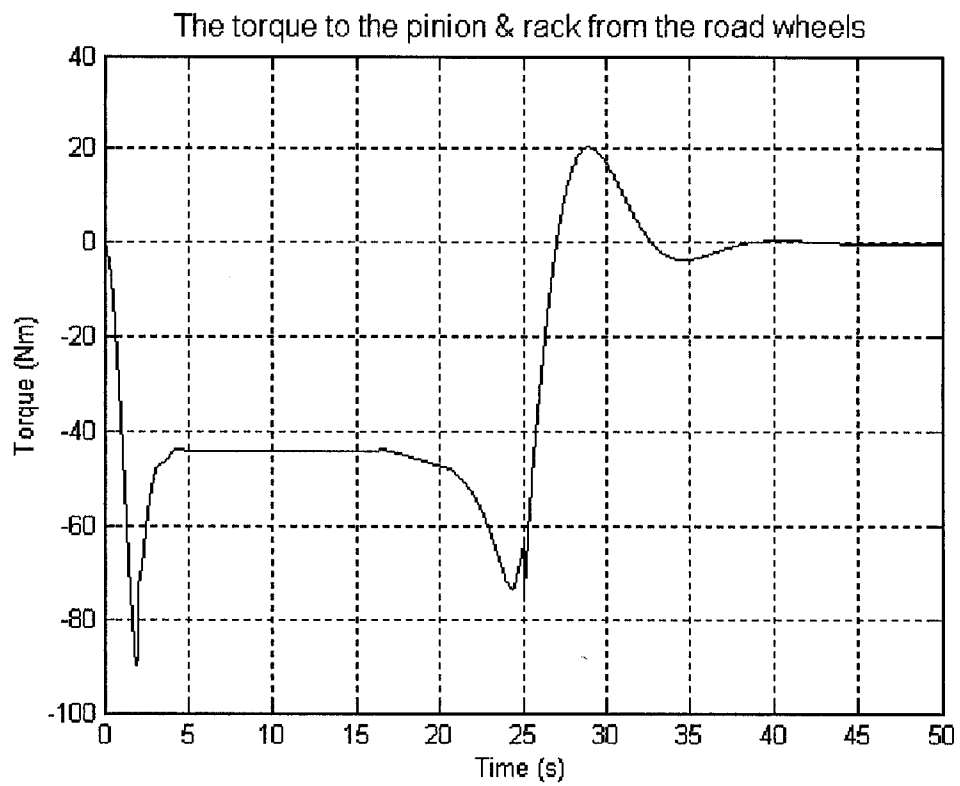


Figure 3-7: The torque on rack and pinion generated from front wheels

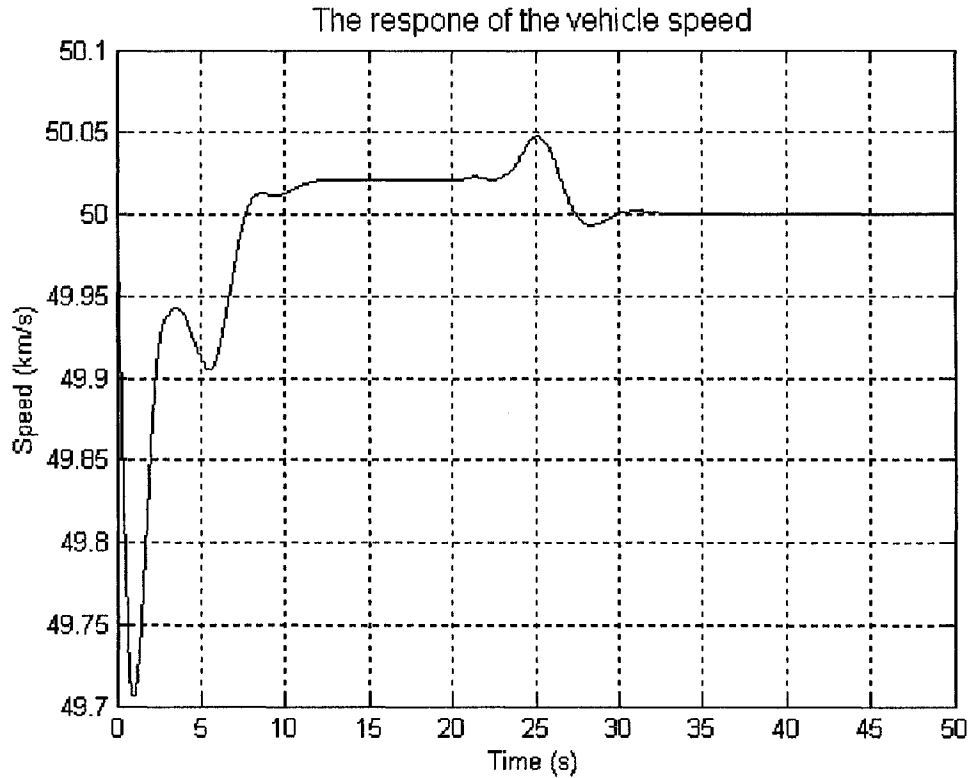


Figure 3-8: The response of the vehicle speed

3.5.5 CONCLUSION

Those plots shown in the preceding section indicate that there is minus difference, in the time response, between the commercial model of CarSim™ and the proposed model. Also expected and acceptable is the error between the commercial and proposed dynamic models. The proposed model can be used for the model based controller design for the EPS system and the following simulation.

As mentioned in [13] and [15], the most important requirement for the EPS system is the frequency reflection between the rack force and the reaction torque. The other requirement is to ensure conventional power steering performance. That is to say, the requirement is sufficient assist force at very low frequency. As shown in the plots, the EPS system with a conventional PI controller cannot achieve such requirements.

CHAPTER 4:TWO-DEGREE FREEDOM CONTROLLER DESIGN

4.1 INTRODUCTION

As the literature survey indicated, the most promising EPS controllers are developed based on motor control with some compensators. However, these controllers have their own limitations, and the design is complex. The reaction to the torque from road wheel is one of the most important issues in the development of EPS control system. The problem is how to design a controller to reject external disturbances and provide proper steering feel. From the research in [46], the high frequency part of the road wheel torque is treated as the unnecessary information or disturbance and the low frequency part is the necessary information, which need to be transmitted to the driver properly. The traditional controller architecture has its own limitation for this.

In this chapter, new controller architecture is proposed. The design of the EPS control unit is divided into two independent stages, motor controller design and motion controller design. First, a motor controller is designed to achieve a fast reaction speed. And then, a robust controller is designed using H_∞ technology, based on the proposed controller architecture and the EPS model presented in chapter 3. With the new controller, the necessary information is emphasized and the unnecessary information is partially rejected.

The remainder of this chapter is organized as follows. Section 4.2 contains the design specifications. In section 4.3, an abstracted model is derived from the model presented in chapter 3 to address the steering feel problem. And then, the new controller architecture is proposed in section 4.4. The design of a PI motor controller and a H_∞ motion controller are presented in section 4.5 and 4.6, respectively. The system reliability is analyzed in section 4.7. Section 4.8 contains the conclusion and discussion. Section 4.9 is a special topic to show that PID controller is not suitable for the motion controller.

4.2 DESIGN SPECIFICATIONS

In an EPS system, the assist torque is generated by an electric motor. The control system control the electric motor based on driver's maneuvers, road conditions and motor

status. The basic requirement is that the EPS system must supply sufficient assist torque and the whole system must run under the driver's manoeuvres.

As mentioned in [47], the most important requirement for the EPS system is frequency rectification between the rack force and the torque feedback to the driver. The other requirement is to ensure conventional PS performance (i.e., sufficient assist force at very low frequencies).

As a result, the following design specifications were determined for the EPS systems:

1. The reaction torque should be sensitive to the necessary information from the road, which is the low frequency part of the road wheel torque,
2. The reaction torque should be non-sensitive to the unnecessary information from the road, which is the high frequency part of the road wheel torque,
3. The cut-off frequency is determined as 15Hz [47],
4. The EPS system must generate sufficient assist torque,
5. The vehicle must be turned under driver's manoeuvres.

4.3 SYSTEM MODEL

4.3.1 BLOCK DIAGRAM

Figure 4-1 shows a conventional control block diagram of the EPS system.

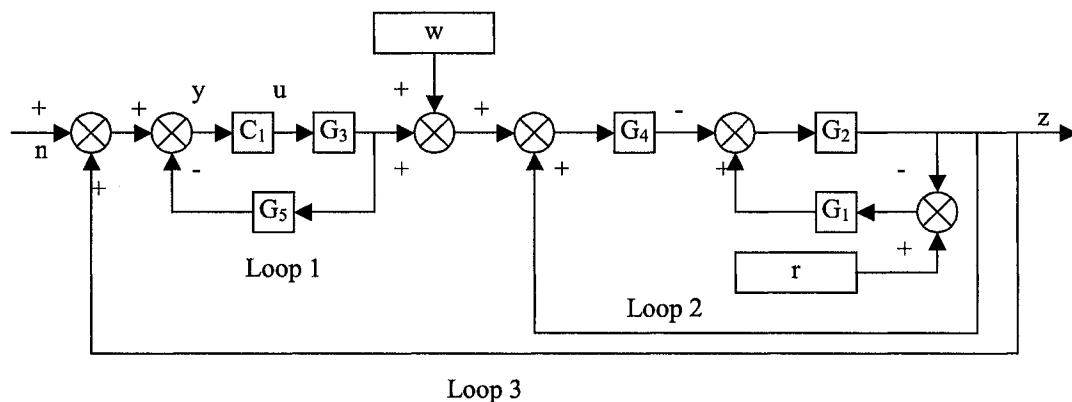


Figure 4-1: EPS System Block Diagram

In the figure, the following nomenclature is used:

- C_1 : motor controller
- G_1 : hand wheel dynamics

- G₂: torque sensor block
- G₃: BDC motor dynamics
- G₄: rack and pinion dynamics
- G₅: current sensor block
- w: disturbance torque from road
- r: torque from driver to the hand wheel
- z: torque feedback to the driver through hand wheel
- u: the control signal
- y: the measured error signal, or controller input
- n: torque sensor noise
- Loop1: motor feedback control loop
- Loop2: road wheel torque loop
- Loop3: steering feedback loop

4.3.2 STATE SPACE MODEL

The state space model is necessary to design a model-based controller. The general format of the state space model is:

$$\begin{aligned}\dot{\mathbf{x}} &= \mathbf{A}\mathbf{x} + \mathbf{B}_1\mathbf{w} + \mathbf{B}_2\mathbf{u} \\ \mathbf{z} &= \mathbf{C}_1\mathbf{x} + \mathbf{D}_{11}\mathbf{w} + \mathbf{D}_{12}\mathbf{u} \\ \mathbf{y} &= \mathbf{C}_2\mathbf{x} + \mathbf{D}_{21}\mathbf{w} + \mathbf{D}_{22}\mathbf{u}\end{aligned}$$

where

- x**: state vector
- w**: the disturbance signal
- u**: control signal from controller
- z**: the performance signal
- y**: the measured error signal
- A**: the system matrix
- B** = [**B**₁ **B**₂]: the input matrix
- C** = [**C**₁
C₂]: the output matrix

$$\mathbf{D} = \begin{bmatrix} \mathbf{D}_{11} & \mathbf{D}_{12} \\ \mathbf{D}_{21} & \mathbf{D}_{22} \end{bmatrix}: \text{ feed-forward matrix}$$

For the presented EPS model, as shown in Figure 4-1,

$$\mathbf{A} = \begin{bmatrix} 0 & 1 & 0 & 0 & 0 & 0 \\ -151.5 & -0.7 & 0 & 0 & 151.5 & 0.0947 \\ 0 & 0 & 0 & 1 & 0 & 0 \\ 0 & 0 & -38 & -12 & 0 & 0 \\ 0 & 0 & 0 & 0 & 0 & 1 \\ 2597.4 & 1.623 & 3896.1 & 11688.3 & -2597.4 & 17.86 \end{bmatrix}$$

$$\mathbf{B} = [\mathbf{B}_1 \quad \mathbf{B}_2] = \begin{bmatrix} 0 & 0 \\ 0 & 0 \\ 0 & 0 \\ 0 & 1 \\ 0 & 0 \\ 32.47 & 0 \end{bmatrix}$$

$$\mathbf{C} = \begin{bmatrix} \mathbf{C}_1 \\ \mathbf{C}_2 \end{bmatrix} = \begin{bmatrix} 80 & 0.05 & 0 & 0 & -80 & -0.05 \\ 80 & 0.05 & -0.5 & -1.5 & -80 & -0.05 \end{bmatrix}$$

$$\mathbf{D} = \begin{bmatrix} \mathbf{D}_{11} & \mathbf{D}_{12} \\ \mathbf{D}_{21} & \mathbf{D}_{22} \end{bmatrix} = \begin{bmatrix} 0 & 0 \\ 0 & 0 \end{bmatrix}$$

The state space model shows that neither of \mathbf{D}_{12} and \mathbf{D}_{21} are full rank. \mathbf{C}_1 is not a good position to control the disturbance signal, w .

4.4 NEW CONTROLLER ARCHITECTURE

In my research, a controller is designed, to minimize the noise from the road, while transfer the necessary information to the driver. The controller architecture shown in Figure 4-1 has some disadvantages:

1. The disturbance signal, w , is in the steering feedback control loop (loop 3), but the controller is in motor feedback control loop (loop 1). As a result, the controller is not sensitive to the disturbance signal.
2. The motor can be modelled as a low pass filter because of its inertia moment and friction. It can be difficult for the controller to do complicated behaviour.

3. Motor control is a complicated topic if the implementation strategy is considered. The controller design becomes more complicated if the controller can control the motor efficiently and formulate the motion of the system at the same time.
4. The whole controller has to be redesigned if the motor is changed and it is possible that the new controller cannot be implemented.

New controller architecture, as shown in Figure 4-2, is proposed to simplify the control design procedure without any cost penalty. In Figure 4-2, block M denotes the motor assembly including the motor controller, as shown in Figure 4-3. G is the mechanical plant to be controlled, as shown in Figure 4-4. And C_2 is the proposed extra controller.

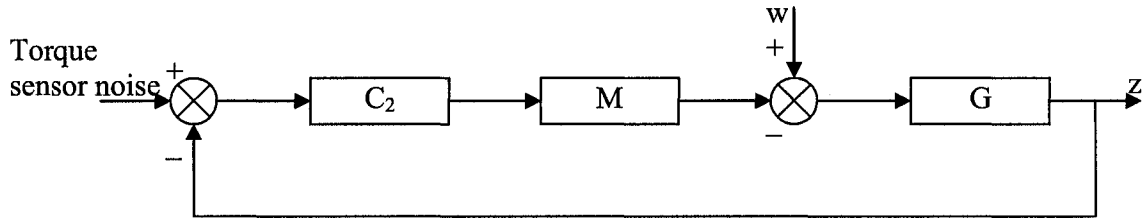


Figure 4-2: New Control Architecture With Motion Controller

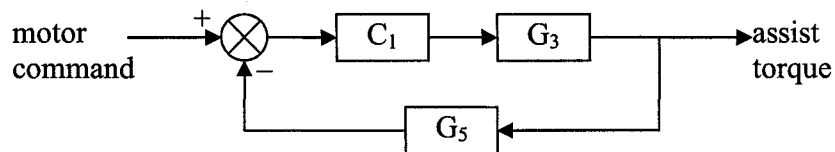


Figure 4-3: Motor Control Assembly

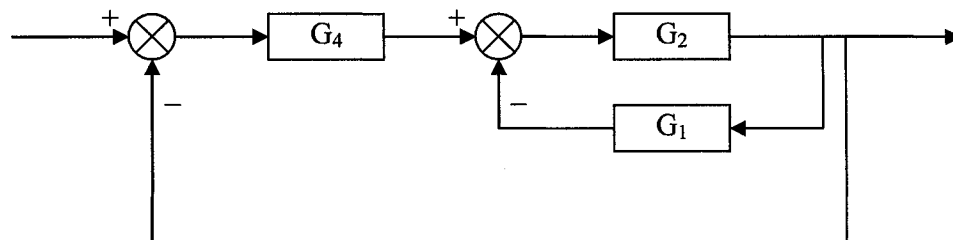


Figure 4-4: Controlled Plant

In the proposed control architecture, another controller C_2 , say motion controller, is introduced to do the motion control of the whole system. The main advantage is that the new controller can directly control the motion of the system without the consideration of the detail of motor control, and the controller within motor feedback control loop, loop 1, can do motor control without the consideration of the motion specification of the system. As a result, the system design can be separated into two stages, which are:

1. Motor control design
2. System motion control design

4.5 MOTOR CONTROLLER DESIGN

4.5.1 MOTOR CONTROL SYSTEM DESCRIPTION

Figure 4-3 shows the motor control diagram. In the diagram, C_1 denotes the motor controller, and G_3 and G_5 denote the motor model and current feedback sensor, respectively. From the knowledge of brushed DC motor, the motor current is proportional to the output torque. In my model,

$$G_3 = \frac{60s + 20}{s^2 + 12s + 38}$$

and

$$G_5 = \frac{1}{40}$$

So the problem of motor torque control can be translated to motor current control and the feedback current is used to measure the motor output torque.

4.5.2 PI CONTROLLER DESIGN

Most of the motors use PI controller to control the output torque, motor speed or both. The reason why D controller is not popular is that the motor control system is an over-damping system, and D controller will reduce the reaction speed. The slow reaction speed can also worsen the system stability. In my case, the PI controller is designed to reduce the rising time in the system step response. Figure 4-5 shows the step response of the motor module with two sets of PI coefficients.

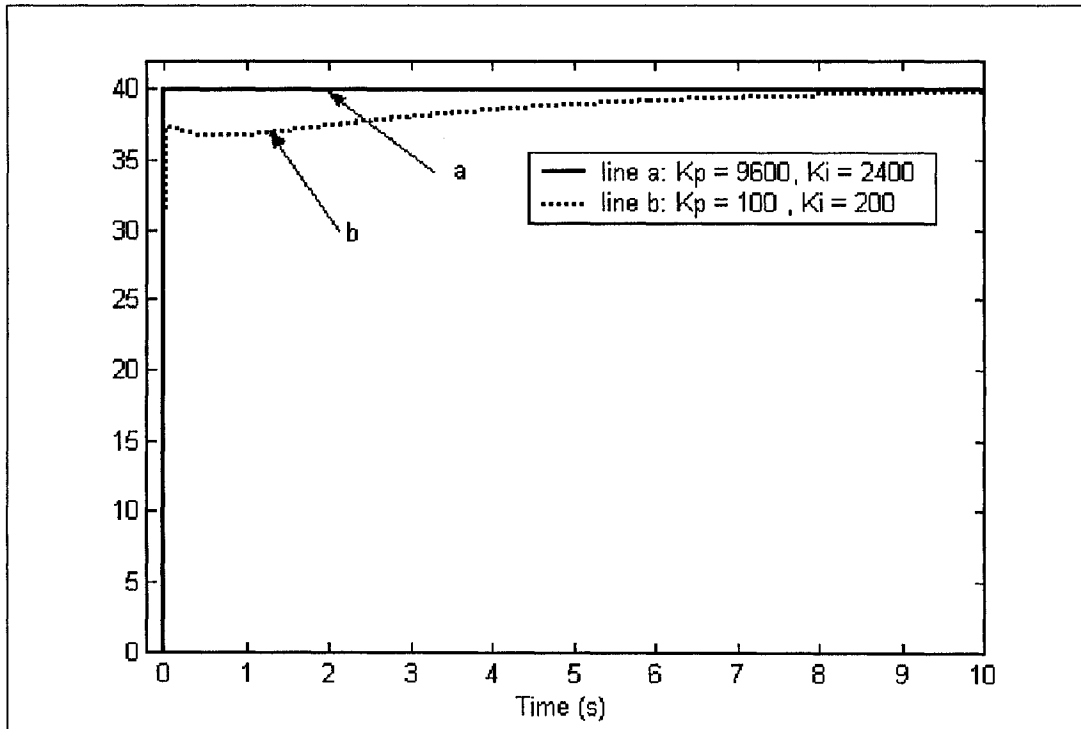


Figure 4-5: the Step Response with Two PI Controllers

From this diagram, one can see that, to compare with line b, line a has less rising time, and both lines have the same steady value, which is 40, or $1/G_5$. It can be concluded that it is possible to control the assist gain by adjusting the value of G_5 .

4.6 H_∞ CONTROLLER DESIGN

4.6.1 SYSTEM AUGMENTATION

Figure 4-6 shows the augmented plant to integrate the specifications in the previous section. The following nomenclature is used in figure 4-6:

- w: the disturbance signal from road wheel torque;
- C_2 : the H_∞ controller to be designed;
- M: the motor module with a PI controller, as shown in Figure 4-3;
- G: the plant as shown in Figure 4-4;
- W_1 : weight function expressing specification 1;
- W_2 : a small number to ensure a full rank D_{12} as required by MatLab routine `hinf` [45];
- W_3 : weight function expressing specification 2.

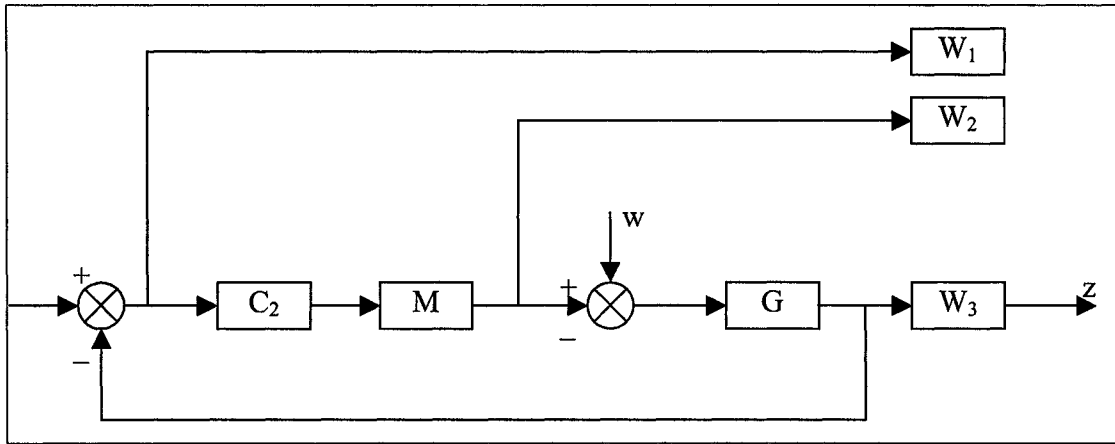


Figure 4-6: Plant Augmentation

The weighting strategy integrating the design specifications is shown in Figure 4-7. W_1 can be also called sensitivity function. To make the system sensitive to low frequency part of the road wheel torque signal, which is below the cut off frequency of 15Hz, W_1 is selected as a low pass filter with the cut off frequency of 15Hz.

$$W_1 = \gamma \frac{10^6}{s^3 + 200s^2 + 2 \times 10^4 s + 10^6}$$

where γ is 1 for the first try, and then can be increased accordingly later.

To minimize the infinity norm for the high frequency signal of road wheel torque to the reaction torque, W_3 is selected as a high pass filter.

$$W_3 = \frac{s}{100}$$

Let assume the signal r is zero, the state-space model of plant, G , can be calculated as:

$$\mathbf{ag} = \begin{bmatrix} -18.558 & -2761.3 & -4033.8 \\ 1 & 0 & 0 \\ 0 & 1 & 0 \end{bmatrix}$$

$$\mathbf{bg} = \begin{bmatrix} 1 \\ 0 \\ 0 \end{bmatrix}$$

$$\mathbf{cg} = [1.6234 \quad 2598.4 \quad 1574.2]$$

$$\mathbf{dg} = 0$$

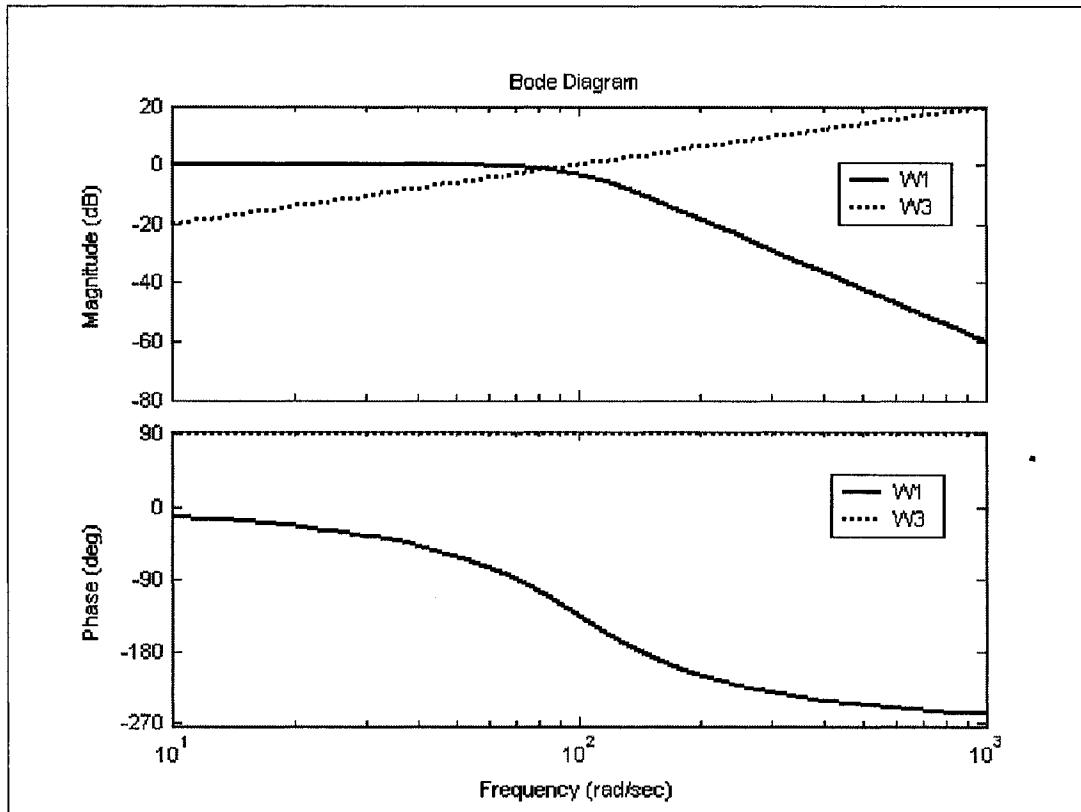


Figure 4-7: Weighting Strategy

To make sure D_{12} is full rank in the augmented plant, w_2 is assigned to 0.01 [45]. MatLab routine *augtf* can be used to do the plant augmentation [45].

4.6.2 H_∞ CONTROL SYNTHESIS

The so-called H_∞ Small-Gain Problem can be solved using the numerically robust descriptor 2-Riccati formulae of [46]. The parameter γ of W_1 is the only parameter on which is iterated for design; the Robust Control Toolbox script-file *hinftopt.m* automates this iteration.

Figure 4-8 shows the output, which appears on the screen for the result of γ -iteration. Figure 4-9 shows the output, which appears on the screen for a successful run of *hinf.m*.

<< H-Infinity Optimal Control Synthesis >>

No	Gamma	D11<=1	P-Exist	P>=0	S-Exist	S>=0	lam(PS)<1	C.L.
1	1.0000e+000	OK	OK	OK	OK	OK	OK	STAB
2	2.0000e+000	OK	OK	OK	OK	OK	OK	STAB
3	4.0000e+000	OK	OK	FAIL	OK	OK	OK	UNST
4	3.0000e+000	OK	OK	FAIL	OK	OK	OK	UNST
5	2.5000e+000	OK	OK	FAIL	OK	OK	OK	UNST
6	2.2500e+000	OK	OK	OK	OK	OK	OK	STAB
7	2.3750e+000	OK	OK	FAIL	OK	OK	OK	UNST
8	2.3125e+000	OK	OK	FAIL	OK	OK	OK	UNST
9	2.2813e+000	OK	OK	FAIL	OK	OK	OK	UNST
10	2.2656e+000	OK	OK	OK	OK	OK	OK	STAB

Iteration no. 10 is your best answer under the tolerance: 0.0100 .

Figure 4-8: γ -iteration output

<< H-inf Optimal Control Synthesis >>

Computing the 4-block H-inf optimal controller
using the S-L-C loop-shifting/descriptor formulae

Solving for the H-inf controller F(s) using U(s) = 0 (default)
Solving Riccati equations and performing H-infinity
existence tests:

1. Is D11 small enough? OK
2. Solving state-feedback (P) Riccati ...
 - a. No Hamiltonian jw-axis roots? OK
 - b. A-B2*F stable (P >= 0)? OK
3. Solving output-injection (S) Riccati ...
 - a. No Hamiltonian jw-axis roots? OK
 - b. A-G*C2 stable (S >= 0)? OK
4. max eig(P*S) < 1 ? OK

all tests passed -- computing H-inf controller ...
DONE!!!

Figure 4-9: successful H_∞ Control Synthesis

The final H_∞ controller can be derived by the following equation:

$$C = \frac{\bar{C}}{M}$$

where \bar{C} is the 6-order controller calculated by MatLab and M is the transfer function of the motor module. The final controller is an 8-order controller, as shown below:

$$A = \begin{bmatrix} -14792 & -2.12 \times 10^7 & -3.96 \times 10^9 & -3.84 \times 10^{11} & -1.87 \times 10^{13} & -2.18 \times 10^{13} & -7.97 \times 10^{12} & -9.2 \times 10^{11} \\ 1 & 0 & 0 & 0 & 0 & 0 & 0 & 0 \\ 0 & 1 & 0 & 0 & 0 & 0 & 0 & 0 \\ 0 & 0 & 1 & 0 & 0 & 0 & 0 & 0 \\ 0 & 0 & 0 & 1 & 0 & 0 & 0 & 0 \\ 0 & 0 & 0 & 0 & 1 & 0 & 0 & 0 \\ 0 & 0 & 0 & 0 & 0 & 1 & 0 & 0 \\ 0 & 0 & 0 & 0 & 0 & 0 & 1 & 0 \end{bmatrix}$$

$$B = \begin{bmatrix} 1 \\ 0 \\ 0 \\ 0 \\ 0 \\ 0 \\ 0 \\ 0 \end{bmatrix}$$

$$C = [-1346.9 \quad -1.44 \times 10^8 \quad -2.93 \times 10^{10} \quad -2.97 \times 10^{12} \quad -1.45 \times 10^{14} \quad -1.66 \times 10^{14} \quad -5.97 \times 10^{13} \quad -6.83 \times 10^{12}]$$

$$D = 7.97$$

4.7 STABILITY ANALYSIS

One of the ways to analyze the stability of the system is to calculate the eigenvector of the system state matrix. The system is rebuilt with the designed H_∞ controller, as shown in Figure 4-2. The state matrix, A , of the system is:

$$A = \begin{bmatrix} -18.558 & -2761.3 & -4033.8 & 0 & 0 & 0 & 1224.5 & 28.449 & 0.319 & 5.0144 & -17.051 & 3481.8 \\ 1 & 0 & 0 & 0 & 0 & 0 & 0 & 0 & 0 & 0 & 0 & 0 \\ 0 & 1 & 0 & 0 & 0 & 0 & 0 & 0 & 0 & 0 & 0 & 0 \\ -1.6234 & -2598.4 & -1574.2 & -200 & -20000 & -1 \times 10^6 & 0 & 0 & 0 & 0 & 0 & 0 \\ 0 & 0 & 0 & 1 & 0 & 0 & 0 & 0 & 0 & 0 & 0 & 0 \\ 0 & 0 & 0 & 0 & 1 & 0 & 0 & 0 & 0 & 0 & 0 & 0 \\ 0 & -0.6892 & -0.4175 & 0 & 0 & 0 & -1361.8 & -5.46 & -0.34 & -5.97 & 18.775 & -3825.2 \\ -0.0106 & -16.97 & -10.281 & 0 & 0 & 0 & 7.97 \times 10^{-4} & -0.6 & -0.011 & -0.182 & 0.562 & -114.11 \\ -2158.9 & -3.5 \times 10^6 & -2.1 \times 10^6 & 0 & 0 & 0 & 343.65 & 0.2736 & -98.66 & 425.08 & 270.97 & 605.05 \\ -25.26 & -40431 & -24494 & 0 & 0 & 0 & 4.02 & 3.2 \times 10^{-3} & -4.63 & -29.413 & 112.6 & -22296 \\ 225.83 & 3.61 \times 10^5 & 2.19 \times 10^5 & 0 & 0 & 0 & -35.947 & -0.0286 & -5.044 & -30.483 & -72.879 & 9011.5 \\ 320.38 & -5.1 \times 10^5 & -3.1 \times 10^5 & 0 & 0 & 50.997 & 0.04 & 1.3512 & -3.992 & -3.992 & -8.7641 & -13255 \end{bmatrix}$$

The eigenvector can be calculated using MatLab routine *eig*. The eigenvector is shown below:

$$eig = \begin{bmatrix} -13156 \\ -1361.8 \\ -82.559 + 101.38i \\ -82.559 - 101.38i \\ -8.5418 + 51.606i \\ -8.5418 - 51.606i \\ -135.01 \\ -1.4743 \\ -0.60602 \\ -50 + 86.603 \\ -50 - 86.603 \\ -100 \end{bmatrix}$$

The eigenvector of the system state matrix shows that all the eigenvalues are in the left-half complex plane, or $\text{Re}(eig) < 0$. So the system is stable.

4.8 DISCUSSION AND CONCLUSION

The frequency characteristics from the road wheel torque to the reaction torque are shown in Figure 4-10.

The bode diagram shows that:

1. for necessary information, lower than 15Hz, the magnitude of the response of H_∞ control system is higher than the traditional control system, and the road feel is enhanced;
2. for disturbance signal, higher than 15Hz, the magnitude of the response of H_∞ control system is lower than the traditional control system, and the disturbance is attenuated.

The bode diagram also shows that the peak response of the system is shifted from the disturbance area to road feel area.

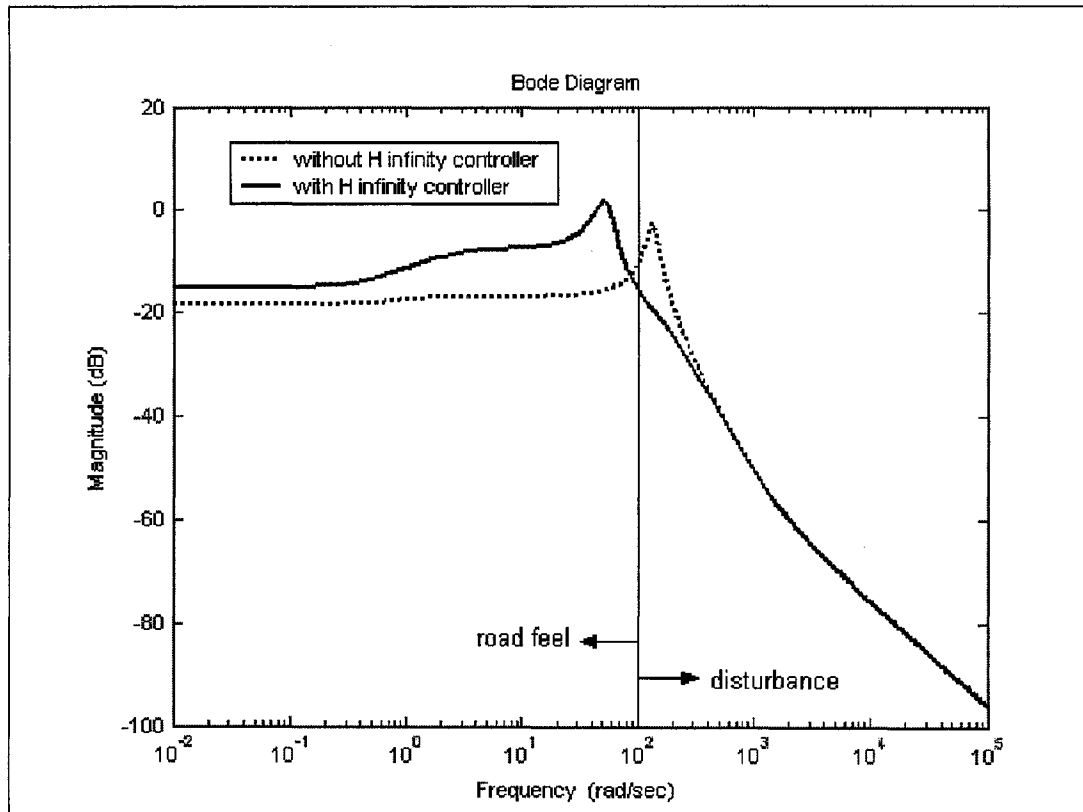


Figure 4-10: Bode diagram for the frequency characteristics from road wheel torque to reaction torque.

4.9 PID MOTION CONTROLLER

PID controllers are always the first choice for close loop control system because of the advantage of easy implementation. The question comes that if it is possible to design a PID controller to do the motion control.

The angle difference between the road tires and steering wheel is measured by the torque sensor. The torque sensor can be treated as a PD controller with proportional gain equal to 80 and derivative gain equal to 0.05. The controllers to be designed, both motion controller for type 1 and type 2 control systems and motor controller for type 3 control system, use this reference signal to determine the value of assist torque. A PID controller is designed using try-error method to increase the system stability margin. First, a PD controller is designed to test the system response of a D controller. Figure 4-11 shows the simulation result of the system using PD as the motion controller.

PD controller also has some problem in implementation and most of the engineers prefer to PI controllers. With try-error method, a PI controller is designed. Figure 4-12 shows the simulation results.

As shown with the arrows in Figure 4-12, there is a sudden turning of the road wheel position, RWP, happened at around 25 seconds after the simulation started. At the same time, there is a sudden jump for torque from road wheel to rack and pinion, RWT, and reaction torque, TRT. The torque from the road wheels to the rack and pinion, RWT, is generated by CarSim and simulates the real torque without any noise. The hand wheel was released after 5 seconds. That is to say, there is no extra signal to the system. The sudden jumps in both RWT and TRT and turn in RWP are generated by the controller. The driver will feel a sudden speed change of the hand wheel, which is a fake road feel. The rack and pinion model shows that the road wheel position has a roughly second order integral relationship with the reaction torque, and the sudden jump is really sharp so that it makes the road wheel have a quick turn. The driver will feel a sudden force change from the steering wheel, which is another fake road feel. The sudden jump increases with the increment of the integral gain.

The simulation shows that PI controller cannot be used as a motion controller for the EPS system.

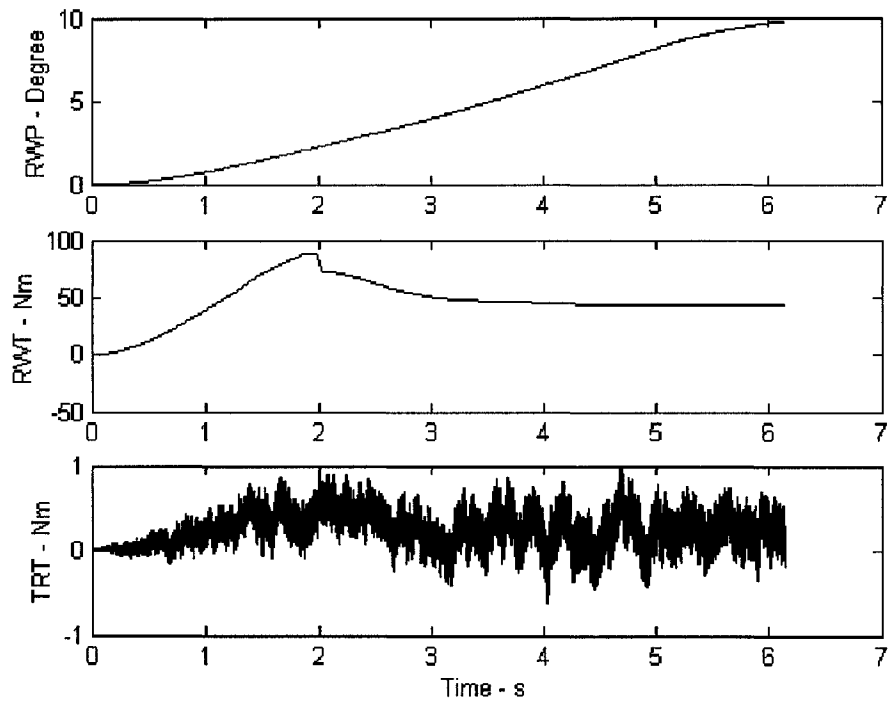


Figure 4-11: using PD motion controller

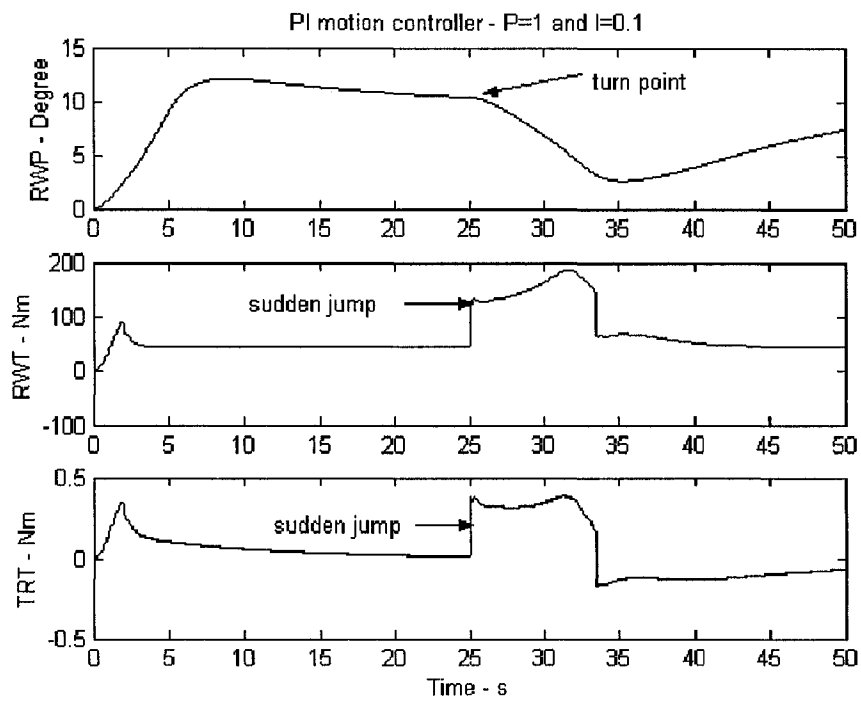


Figure 4-12: Using PI Motion Controller

CHAPTER 5: SIMULATION

5.1 INTRODUCTION

In this chapter, extensive simulation has been made to test the performance of the proposed controller. Some conclusion will be given after the comparison with other control systems.

This chapter is organized as follows. Section 5.2 presents the experimental environment. The simulation result is presented in section 5.3. Based on the simulation results, section 5.4 contains some discussion on the results.

5.2 TESTBENCH

A schematic diagram of the testbench is presented in Figure 5-1.

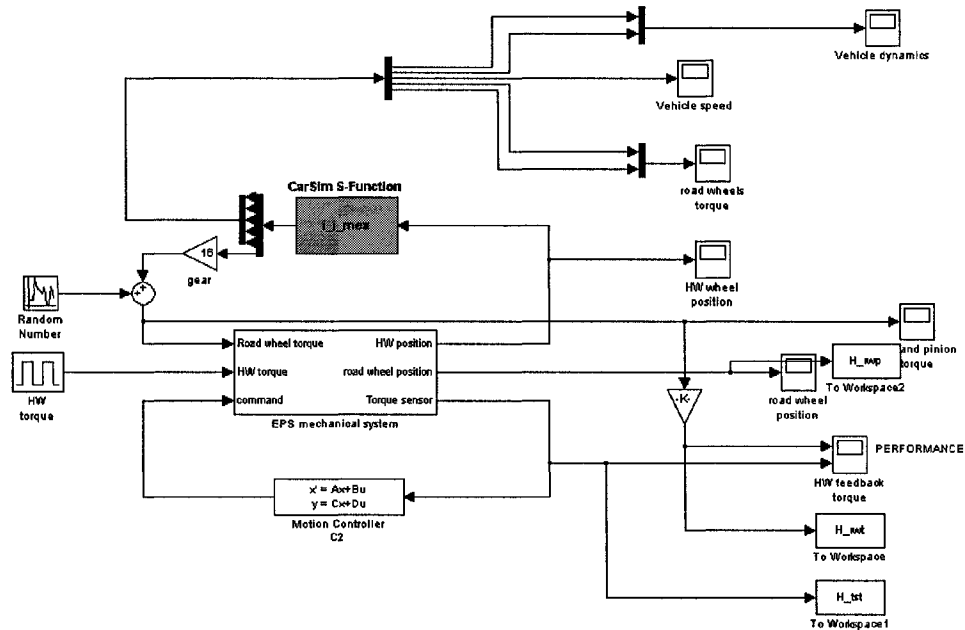


Figure 5-1: Simulation Testbench

The CarSim S-Function denotes a CarSim Module, which works as a virtual car. The same virtual car as that described in section 3.5.3 is used in the simulation. The motor control module is integrated into the block “*EPS mechanical system*”. The controller block here is the motion controller C_2 . If the motion controller C_2 is replaced by a direct connection, the system is changed back to the traditional controller architecture.

In the simulation, three control strategies will be simulated and compared. The three control strategies are listed in table 5-1.

Table 5-1: three control strategies and simulation configurations

Type	Control strategy	C ₂ configuration
1	H _∞ motion controller + motor controller	C ₂ = H _∞ controller
2	PI motion controller + motor controller	C ₂ = PI controller
3	Motor controller only	C ₂ = 1

The block “*HW torque*” is the system input, which is a pulse signal as shown in Figure 3-4. The input simulates a driver manoeuvre of turning the hand wheel with torque of 1Nm for five seconds and then releasing it.

To test the reaction of the controlled system to the disturbance, extra noise signal is added using block “*random number*” and block “*band-limited white noise*” in MatLab/Simulink. Both blocks generate normally distributed noise. Two kinds of noise, bounded noise and white noise, is used to test the system with the different control strategies. The noise signals are listed below:

1. Zero-mean random number noise with variance of 20
2. Zero-mean random number noise with variance of 50
3. Zero-mean random number noise with variance of 100
4. white noise with power of 0.1
5. white noise with power of 1
6. white noise with power of 10

5.3 SIMULATION RESULT DESCRIPTION

Figure 5-2 to Figure 5-7 show the simulation results of noise attenuation performance of type 1 and type 3 control systems with the noise signals listed in section 5.2. Table 5-2 describes the shown simulation results from Figure 5-2 to Figure 5-7. The upper part in each figure, or part (a), is the simulation result for type 1 control system. And the below part, or part (b), is the simulation result for type 3 control system. The following nomenclature is used to label the output signals:

RWP: Road Wheel Position measured in degree

RWT: The torque from road wheel to rack and pinion, measured in Nm

TRT: The reaction torque, which is the torque sensor output, measured in Nm

Table 5-2: the shown simulation results from Figure 5-2 to Figure 5-7.

Figure #	Part a	Part b	noise
5-2	Type 1	Type 3	Zero mean random number with variance = 100
5-3	Type 1	Type 3	Zero mean random number with variance = 50
5-4	Type 1	Type 3	Zero mean random number with variance = 20
5-5	Type 1	Type 3	White noise with power = 10
5-6	Type 1	Type 3	White noise with power = 1
5-7	Type 1	Type 3	White noise with power = 0.1

It is difficult to design a type 2 control system, which uses a PID controller as the motion controller, and the discussion of type 2 control system is presented in section 4.9. The simulation of type 2 control system is shown in section 5.5.

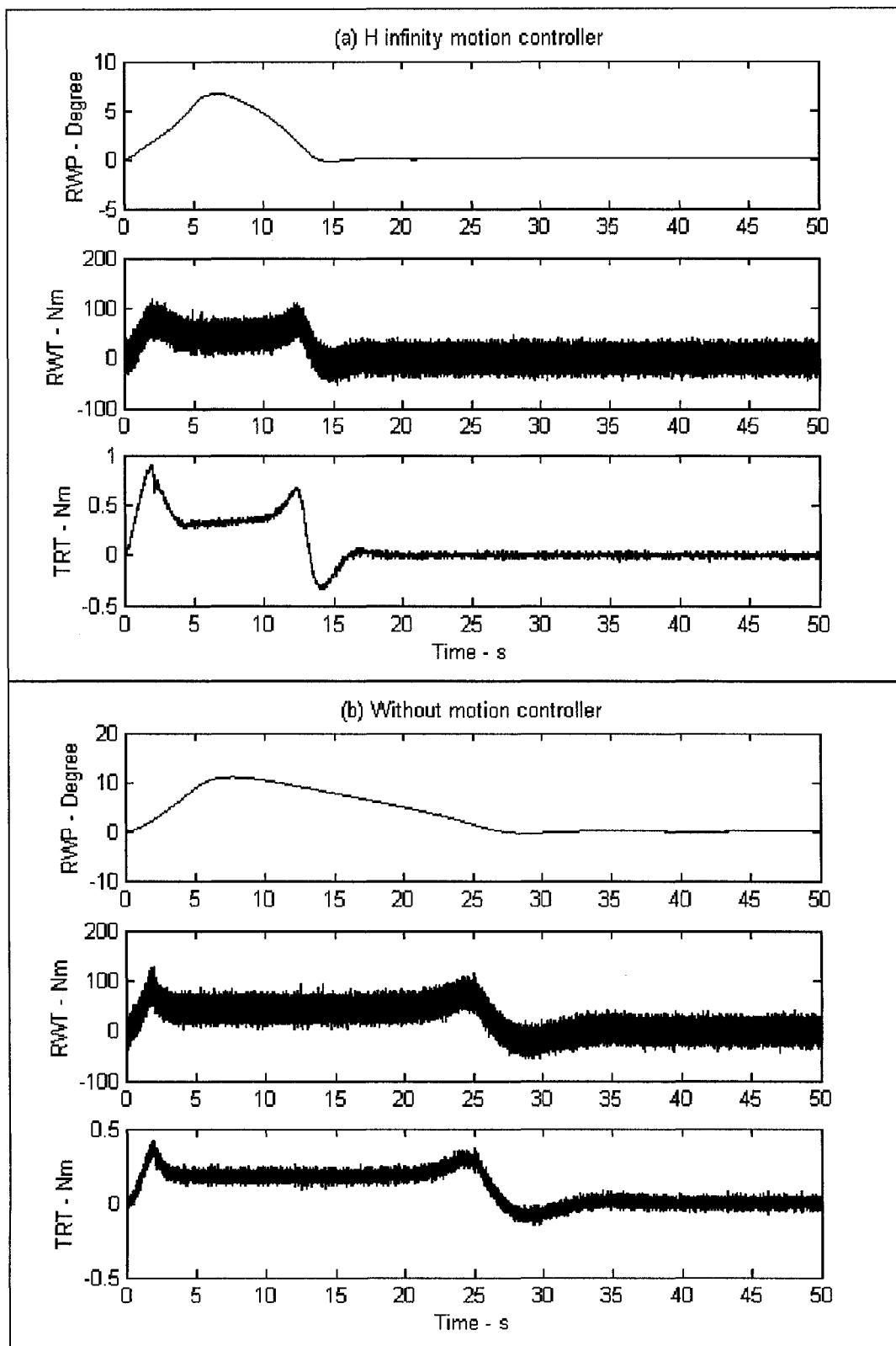


Figure 5-2: Zero Mean Random Number Noise with Variance = 100

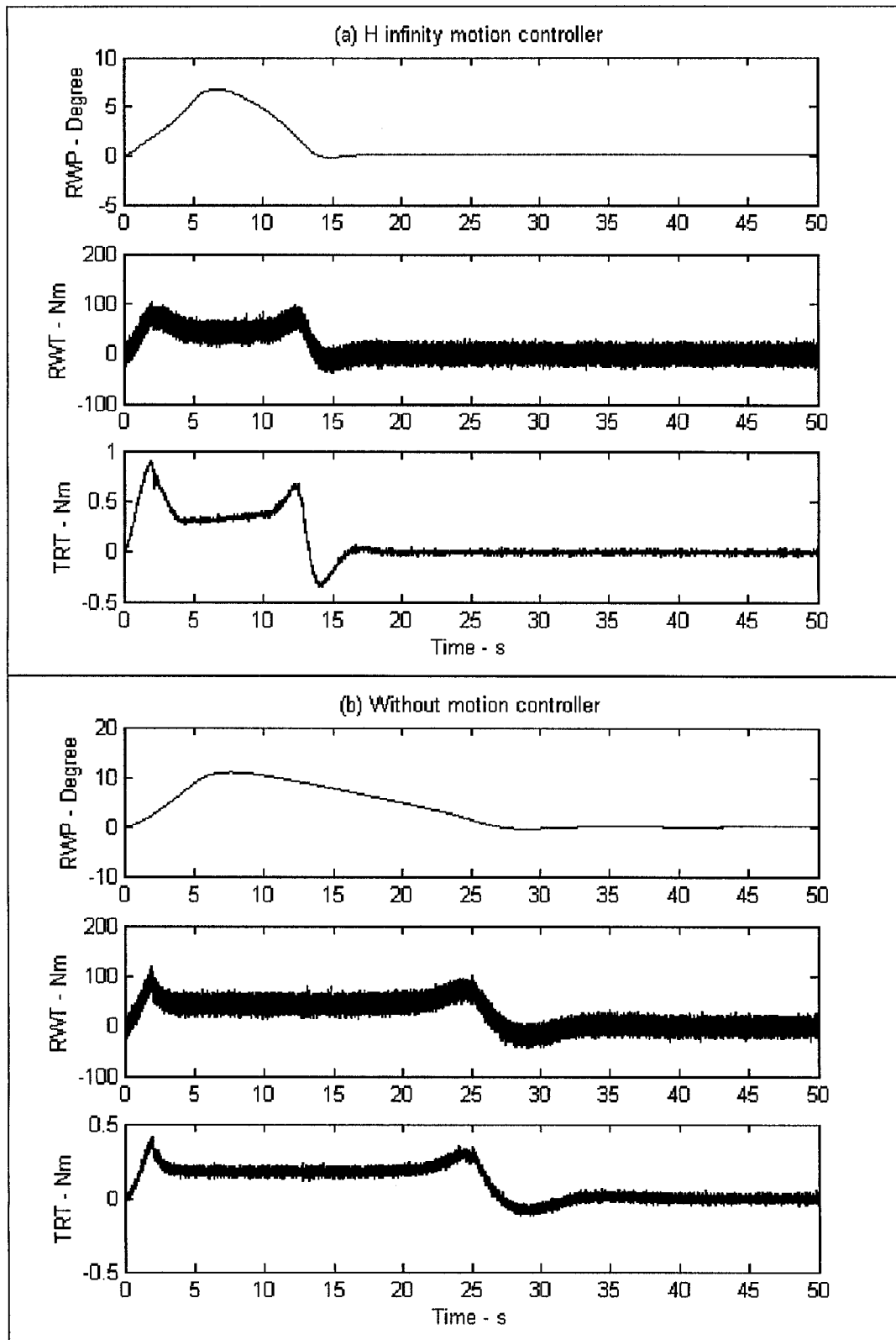


Figure 5-3: Zero-mean Random Number Noise with Variance = 50

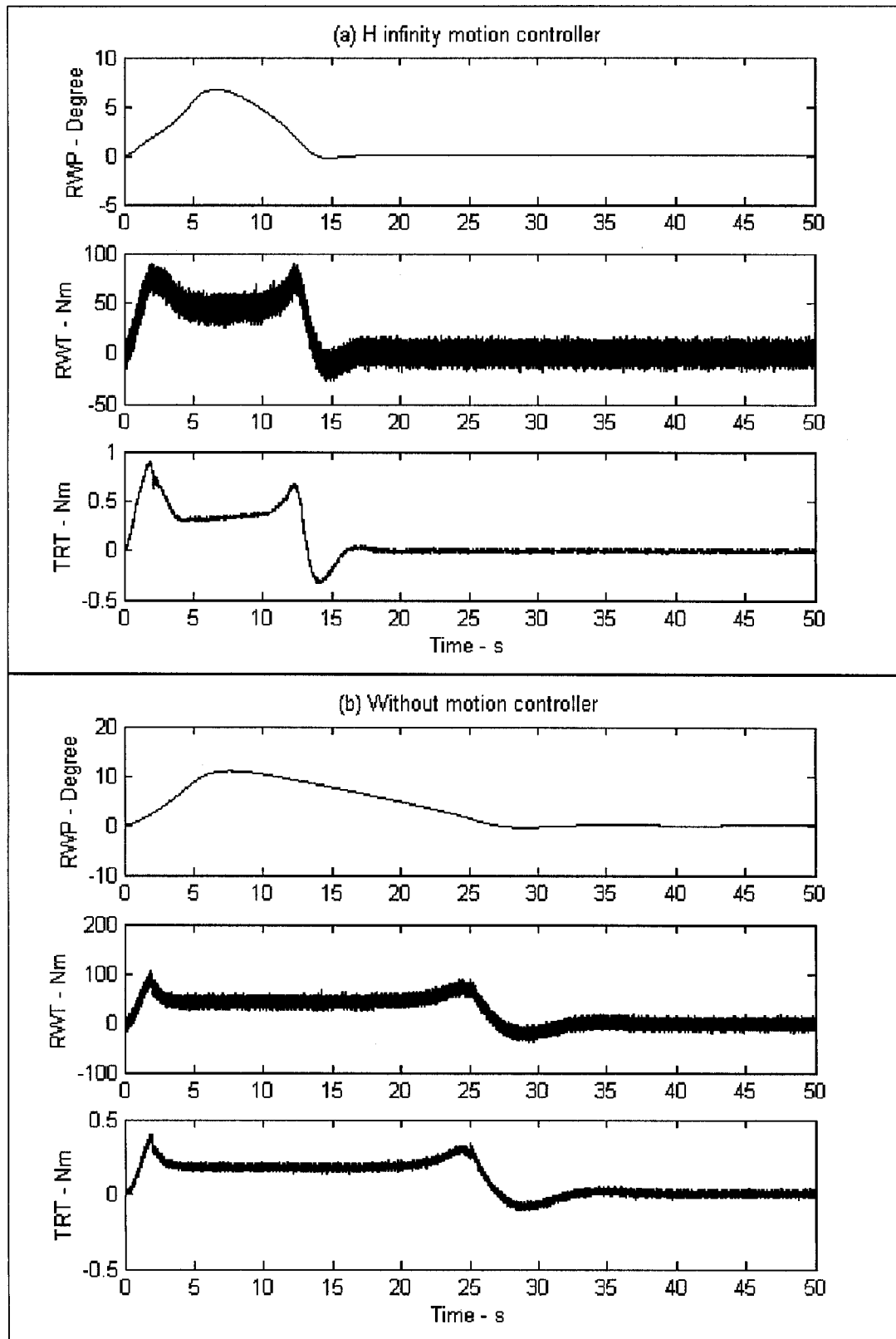


Figure 5-4: Zero-Mean Random Number Noise with Variance = 20

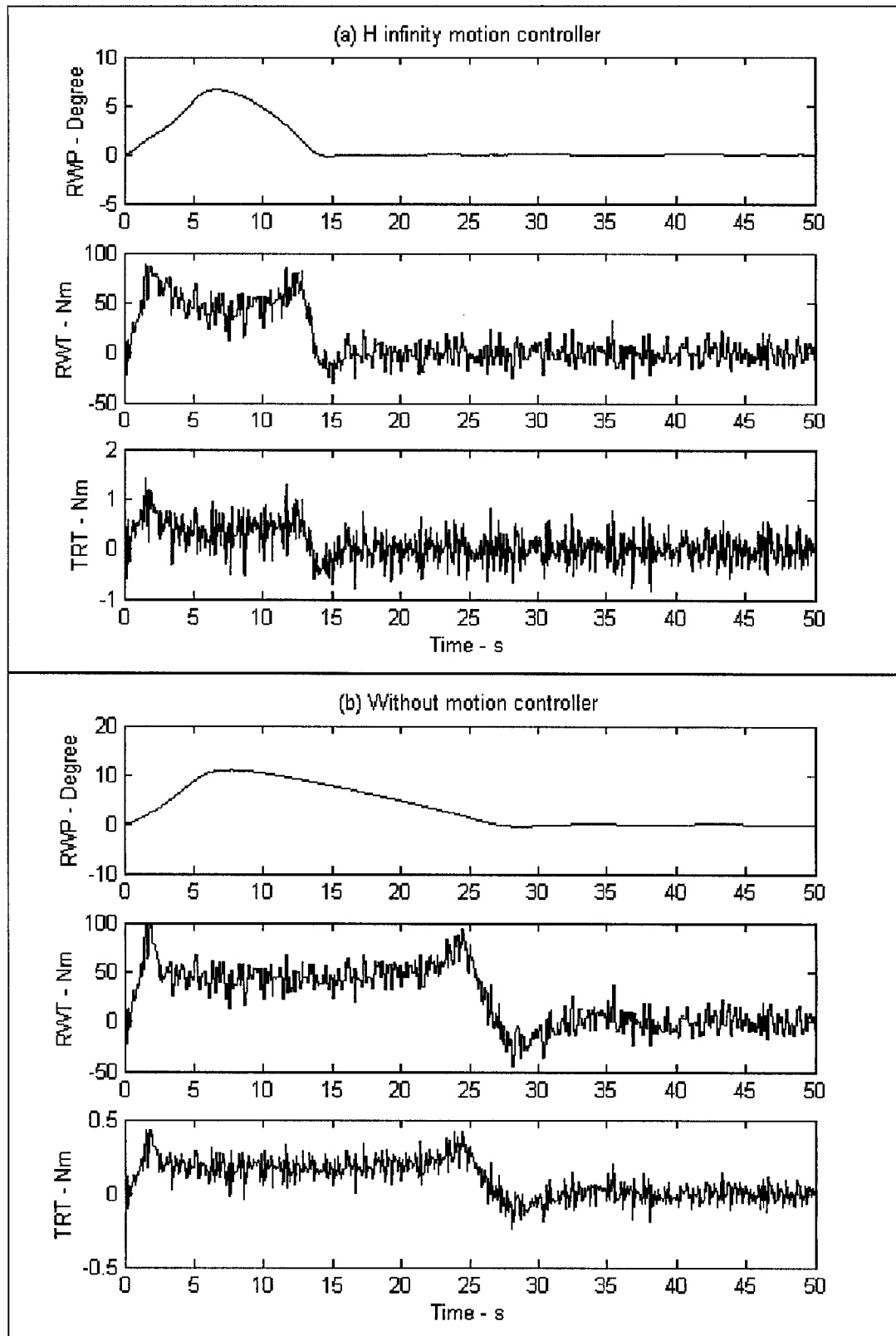


Figure 5-5: White Noise with Power = 10

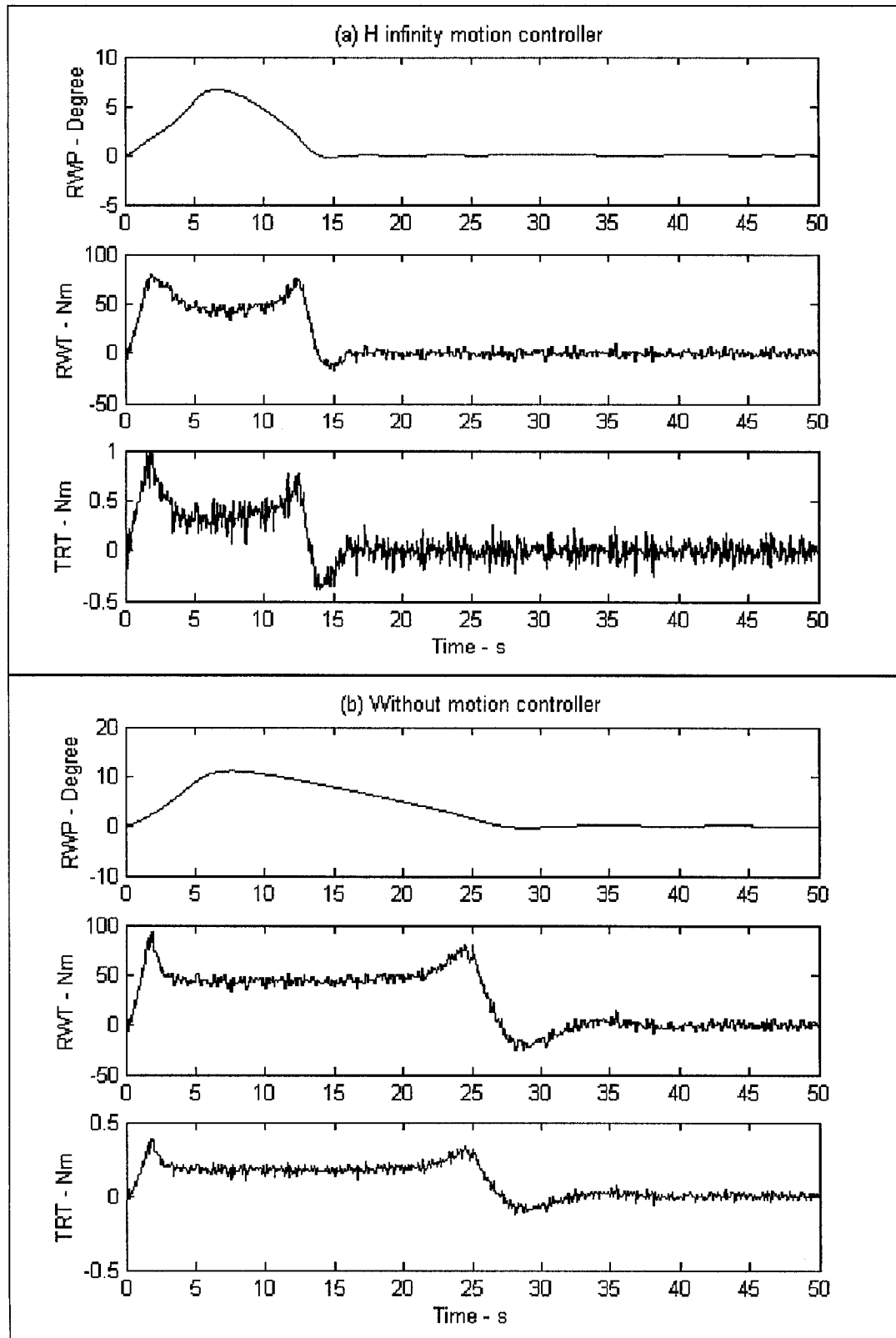


Figure 5-6: White Noise with Power = 1

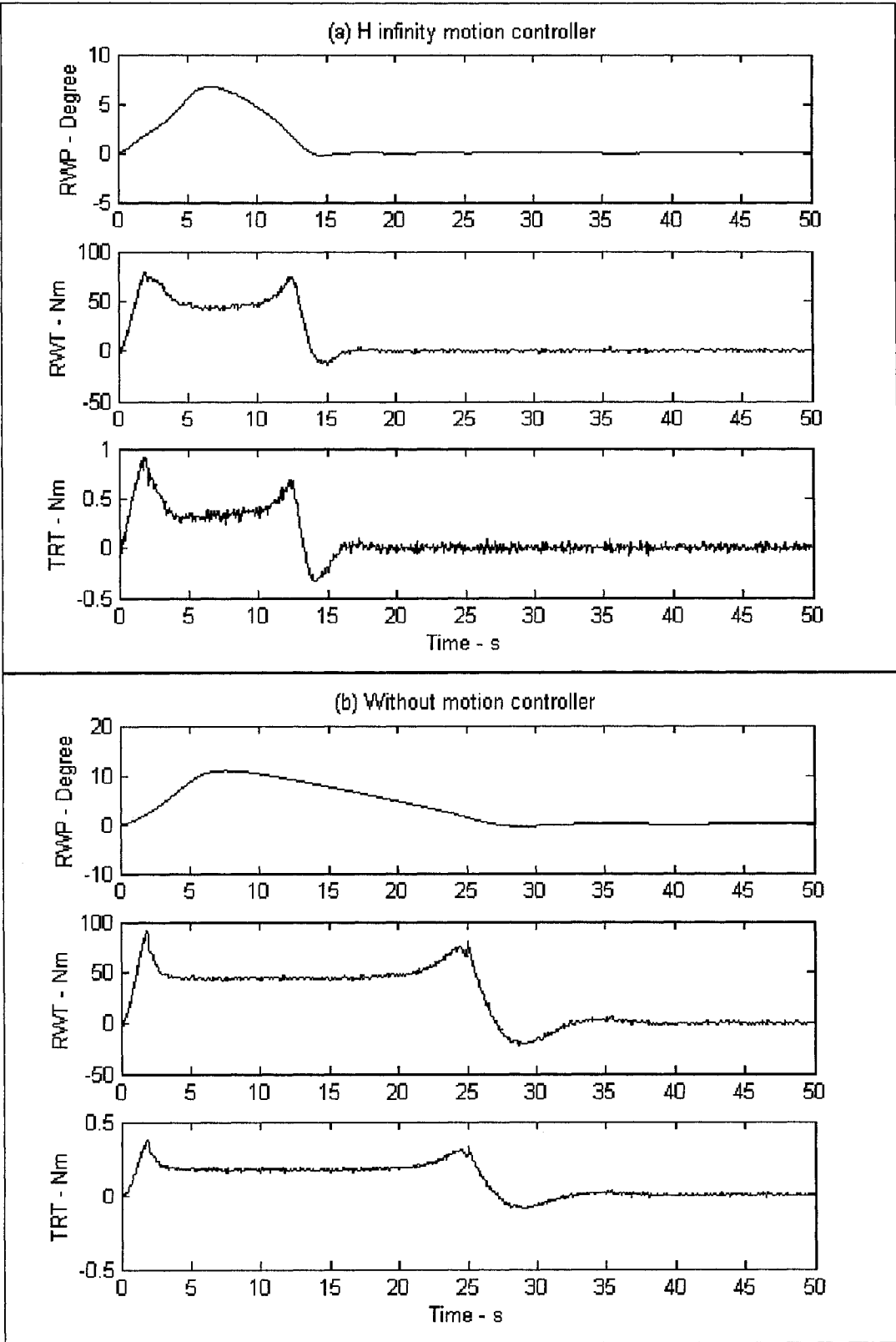


Figure 5-7: White Noise with Power = 0.1

5.4 RESULT DISCUSSION

In the simulation, the speed of the vehicle is set as constant 50km/s. CarSim simulates the behaviours of the vehicle, including the friction between the front tires and the road surface. The RWT (torque from road wheel to rack and pinion) generated by CarSim reflects the real torque in the experimental conditions.

For both of the control systems, H_∞ control system, type 1, and traditional control system, type 3, the basic requirements are satisfied:

1. the front wheels are turned according to the driver's maneuvers and turned back to neutral position after the hand wheel is released, as shown in RWP curve.
2. the driver can obtain sufficient information from the tire/road contact, or the torque to the rack and pinion, RWT, because the reaction torque, TRT, follows the torque to the rack and pinion, RWT.
3. the driver command is amplified by the electric motor.

By comparison between part (a) and part (b) in each figure, one can find out that:

1. If the disturbance is modeled as the bounded noise, as shown in Figure 5.2 to Figure 5.4, the H_∞ controller system can attenuate the noise significantly and enhance the necessary information.
2. On the other hand, if the disturbance is modeled as the white noise, shown in Figure 5.5 to Figure 5.7, the performance of noise attenuation by H_∞ controller system is even worse than the type 3 control system, which is traditional controller system

The following two subsections will discuss the simulation results in more details.

5.4.1 BOUNDED NOISE

For the bounded noise, Figure 5-2 to Figure 5-4, three sets of noise are selected,

- Random number noise with variance = 100, which simulates the very rough road surface with lots of noise
- Random number noise with variance = 50, which simulates the intermediate rough road surface with not too much noise

- Random number noise with variance = 20, which simulates the low rough road surface with little noise

To compare part (a) in each figure from Figure 5-2 to Figure 5-4, one can find out that the reaction torque to the driver, TRT, changes very little. So it can be concluded that the H_∞ control system is not sensitive to bounded noise. To compare part (b) in each of the figures, one can find that the reaction torque, TRT, changes with bound's change of the noise. So it can be concluded that the traditional control system is sensitive to the bounded noise.

5.4.2 WHITE NOISE

For the white noise, Figure 5-5 to Figure 5-7, three sets of noise are selected,

- White noise with power = 10, which simulates the very rough road surface with lots of noise
- White noise with power = 1, which simulates the intermediate rough road surface with not too much noise
- White noise with power = 0.1, which simulates the low rough road surface with little noise

From part (a) in each figure, the H_∞ control system cannot attenuate the white noise. To compare with part (b) in each figure, the performance of H_∞ control systems to attenuate the white noise is worse than that of traditional control systems. One can conclude that H_∞ control system is more sensitive to the white noise than traditional control system.

5.5 PID MOTION CONTROLLER SIMULATION

As discussed in section 4-9, PID controller cannot be used as the motion controller in the presented EPS system. Figure 5-8 to Figure 5-10 show the simulation result of the type 2 control system under the noise described in section 5.2. The simulation results show that the sudden jumps, at 25 seconds after the simulation started, exist in all the noise circumstances. The performance of the noise attenuation is near that of the type 3 control system. So the PID motion controller cannot be used to generate optimized road feel.

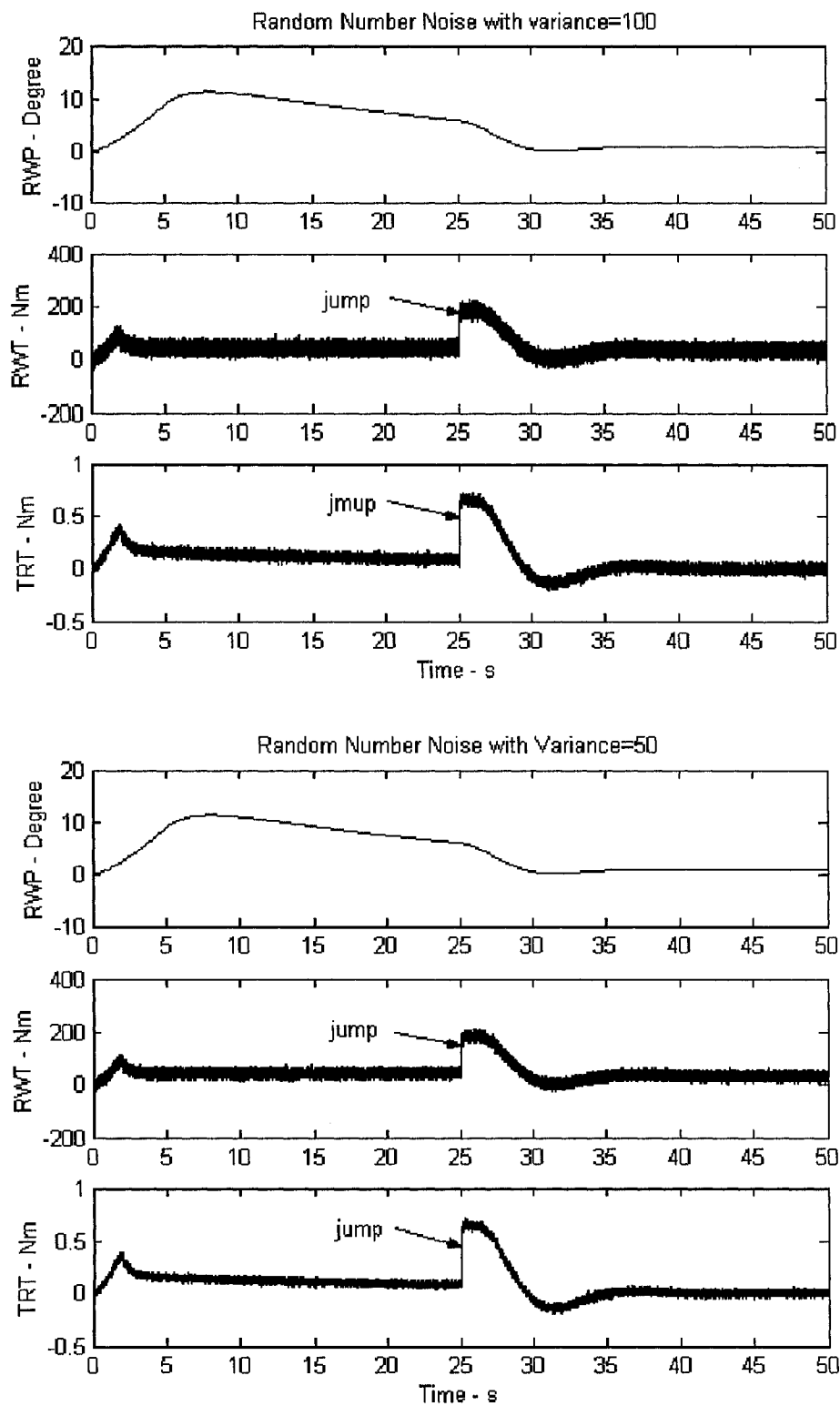


Figure 5-8: Simulation of PID Motion Controller System - 1

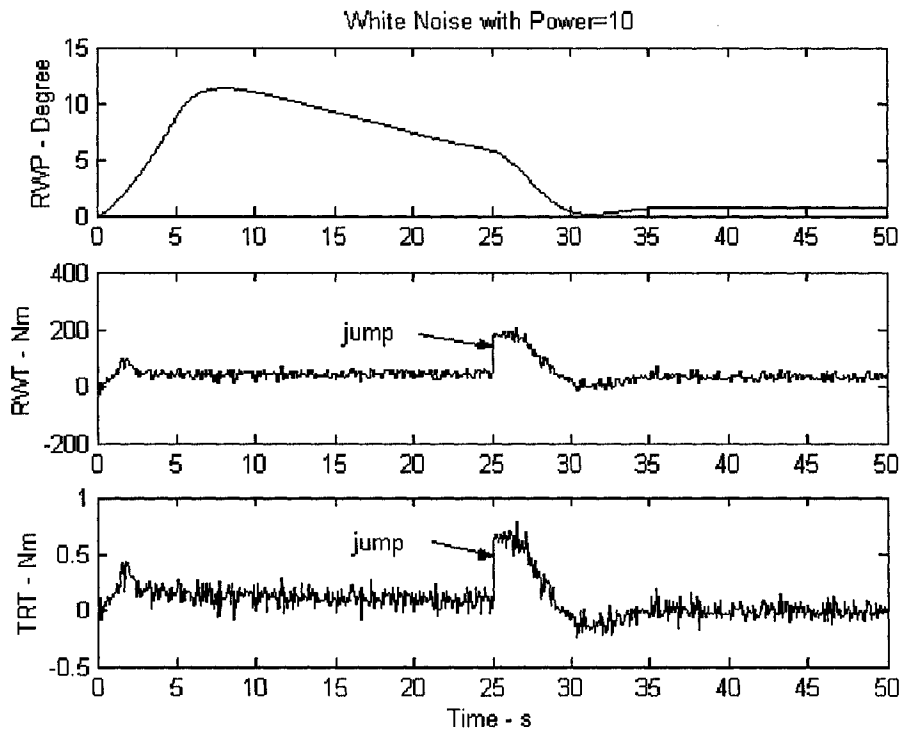
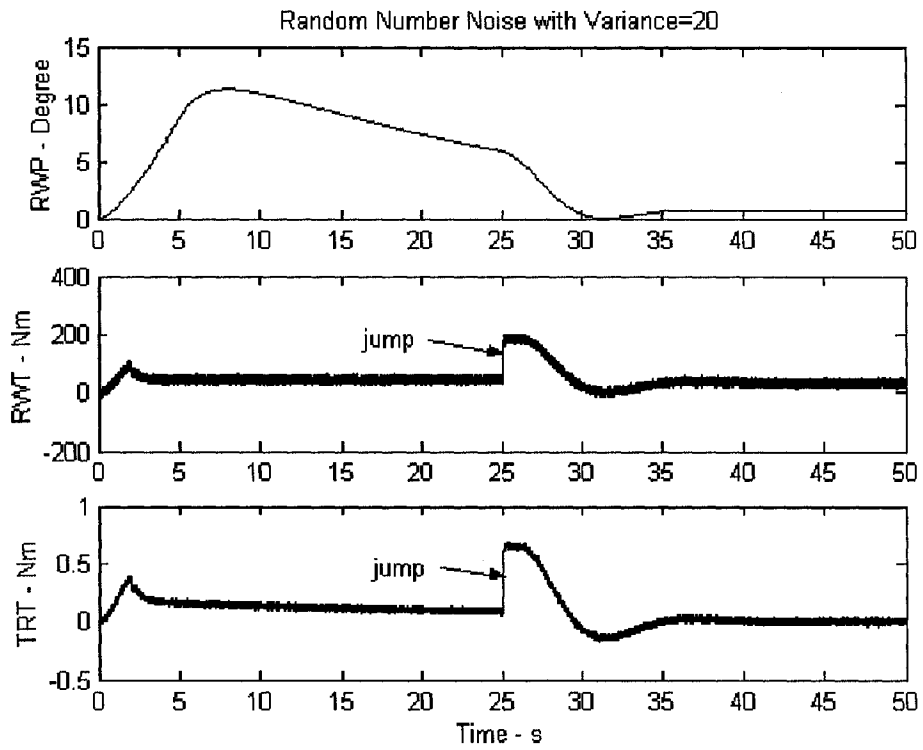


Figure 5-9: Simulation of PID Motion Controller System - 2

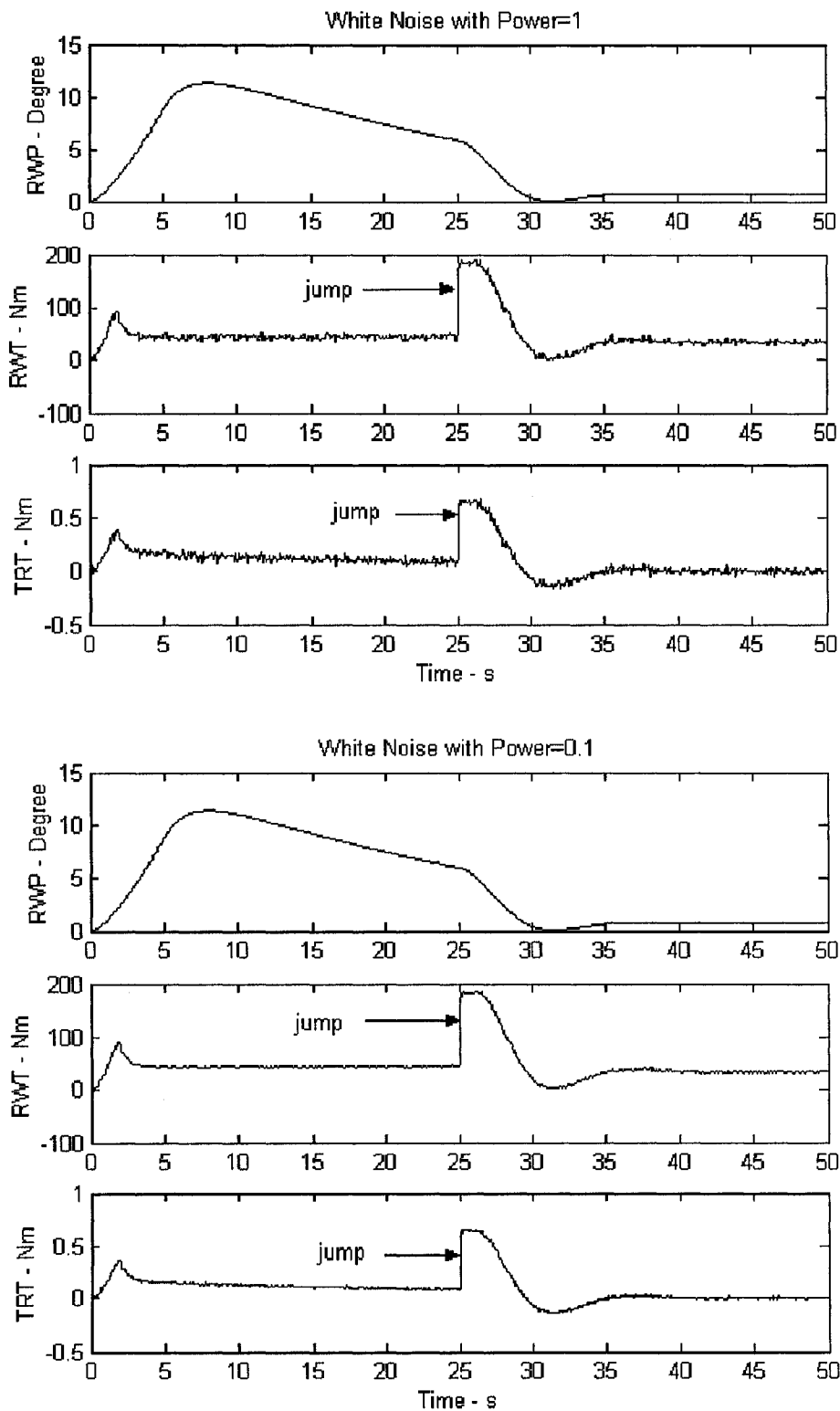


Figure 5-10: Simulation of PID Motion Controller System - 3

CHAPTER 6: CONCLUSIONS

6.1 INTRODUCTION

Previous design for a power steering system has been done to control a hydraulic actuator or electric motor. Several dynamic model and control schemes have been developed to achieve some kinds of design specifications. To reduce the complexity of the design for an EPS control system, new controller architecture is proposed and an H_∞ controller is designed to attenuate the disturbance torque from road to the driver.

This research started with development of EPS model. And based on this model, an H_∞ controller was derived. The designed system satisfies the following requirements:

1. Sufficient assist gain
2. Whole system runs under the driver's manoeuvres
3. Optimum steering feel or road feel
4. Attenuate the disturbance, which is modeled as bounded noise

6.2 DISCUSSION

The dynamic model is derived from the column-type EPS systems. Other types of EPS systems have their own models, which have a little bit difference from the model presented in this thesis. The EPS system can be modeled as a linear multivariable dynamical system, and there are many ways to reduce the order.

The selection of the weight augmentation strategy is very important to derive an H_∞ controller. The transfer functions of the weights have their own constraints and the design specifications have to be translated to some other constraints. It is possible that some of the constraints are conflict with each other. It is inevitable to make some trade-off during the procedure of designing the weighting functions.

In the simulation, the vehicle speed is set as 50km/h. Using CarSim to simulate in various values, it can be found out that the torque from the road tires to the rack and pinion does not change a lot.

6.3 FUTURE WORK

EPS system is one of the safety-critical systems in a model vehicle system. It is also a key component to transmit road feel to the driver. Addition to the control algorithm, a

designer may solve the problems, such as electronics implementation, fail-safe problems, system diagnosis, manufacture and assembly, etc. So, EPS system design is a big topic and new technology emerges every year.

6.3.1 IMPLEMENTATION

A further test of the controller derived in this thesis is a physical implementation on a DSP board with a real time virtual vehicle module. This section describes the experimental setup for this implementation, and some reference design of the proposed controller module in anticipation of this implementation.

6.3.1.1 EXPERIMENTAL SETUP

A schematic diagram of the experimental setup is presented in Figure 6-1. To facilitate discussion, this setup was subdivided into three elements:

1. real time virtual vehicle setup
2. controller
3. PC

Each of these elements will be discussed in detail in the next three sub-sections.

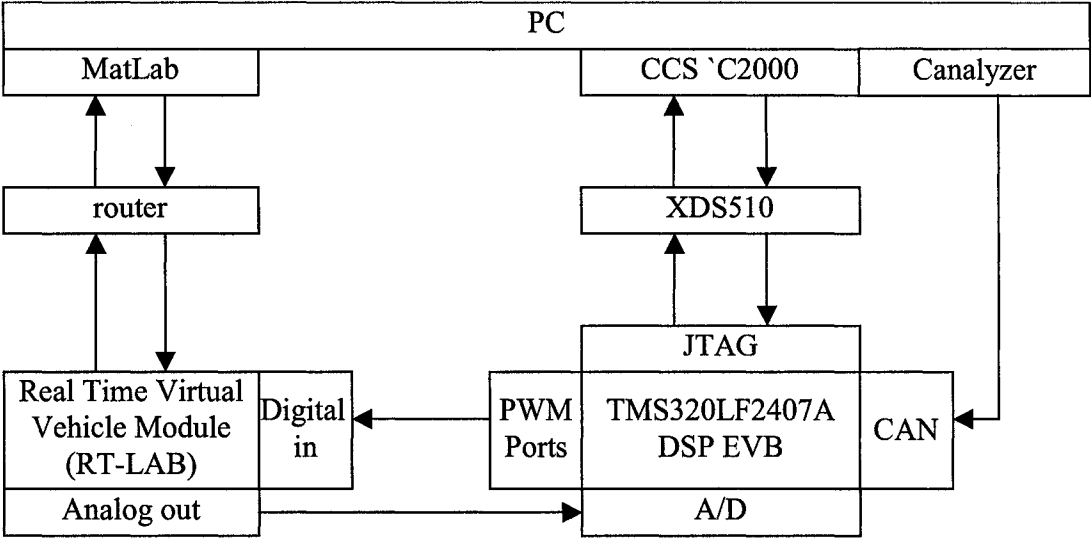


Figure 6-1: Experimental Setup for Controller Test Implementation

6.3.1.2 REAL TIME VIRTUAL VEHICLE SETUP

CarSim is used as the virtual vehicle module. To simulate the real time response of the system, the CarSim module is compiled and loaded into RT-LAB, which is a real time simulation machine.

The real time virtual vehicle module consists of the vehicle module, the EPS module without the controllers and the road surface module. In order to run in real time, the EPS model diagram is modified to get rid of the algebraic loop. The simulation parameters are reconfigured to fit in the real time machine.

The virtual vehicle module accepts the PWM signals from DSP board as motor control signal, and then output the analog signal to the DSP board to simulate the current feedback. The real time machine communicates with PC through a router, so that the program can be downloaded and the simulation results can be displayed in MatLab windows.

6.3.1.3 CONTROLLER

The control algorithm will be programmed into TMS320LF2407A, a DSP made by TI. The chip is embedded within an evaluation board, so that it is not necessary to worry about the I/O ports and power supply for the controller.

At the first stage, speed signal is not necessary in the test because it is assumed that the speed is constant at 50km/s. But the relationship between the vehicle speed and the assist gain is going to be a good topic for future research. So CAN port is reserved to obtain the speed signals.

XDS510 is an in-circuit debugger, which can provide background debug during the simulation process. It communicates with DSP using JTAG and communicates with PC using parallel port. With XDS510, the memory inside the DSP can be monitored and the software can be debugged.

The PWM ports are used to send the motor control signals. The frequency inverter, or motor drive control module, is integrated into the EPS module. The PWM signals are used to drive the virtual electric motor within the EPS module. An on-chip analog to digital converter module is used to receive, from the EPS module, the current feedback signal, which is necessary for the close-loop motor control.

6.3.1.4 PC

The user interacts with the PC to monitor the running of controllers and real time machine. The user can also get the simulation results from the PC. For the purposes of this research, the controller embedded code is written in C with TI libraries. Upon completion, the C code is compiled and downloaded into the DSP memory. During the on-line run, the PC user can monitor the outputs. After that, all the simulation results can be recorded in MatLab.

6.3.2 ORDER REDUCTION

The H_{∞} controller presented is an eight-order controller. To implement the controller, a high performance DSP may be used and the implemented project changes to how to design an efficient matrix multiplier. The question comes: is it necessary to be such a high order controller. Some technology, such as balanced truncation method and Hankel norm approximation method, can be used in this work [44]. But it is also an open question that how to reduce the order while keeping the performance or how much performance can be kept.

6.3.3 MOTOR CONTROL ALGORITHM

Another key work is motor control system design. Frequency inverter is the most popular motor drive system. This system uses PWM signal to switch on/off the power gates to control the voltage on the motor. Although the motor can be treated as a low pass filter, it is inevitable to have some torque ripples.

6.3.4 VARIABLE ASSIST CONTROL

One of the safety topics is how to determine the assist gain in different speed. Variable assist control can be achieved by adjusting the reference signal to the motor system or adjusting the feedback gain within the motor control loop. The desired strategy is to generate low assist torque in high speed to achieve system stability, especially in the road with water or snow, and to generate high assist torque in low speed, for example in the parking lot, to make steering easier.

6.3.5 WHITE NOISE ATTENUATION

As discussed in chapter 5, the H_{∞} controller is very sensitive to the white noise. The problem is how to design a controller to attenuate both bounded noise and statistic noise.

A mix H_2 - H_∞ controller may be a good start because both controllers have similar structures.

CHAPTER 7: BIBLIOGRAPHY

- [1] Anthony, W. Burton, "Innovation Drivers for Electric Power-Assisted Steering," Control Systems Magazine, IEEE , Pages:30 - 39 Volume: 23 , Issue: 6 , Dec. 2003.
- [2] Isamu Chikuma, NSK Ltd., Tokyo, Japan, "Electric Power Steering System," Oct. 3rd, 1995, 5,454,438, US patent.
- [3] H. Shintou, S. Hirakushi, "Technical Trends and Design Improvements of Steering Column", KOYO Engineering Journal English Edition No.161E (2002)
- [4] P. Hingwe, M. Tai and M. Tomizuka, "Modeling and Robust Control of Power Steering System of Heavy Vehicles for AHS," Proceedings of the 1999 IEEE International Conference on Control Applications, August 22-27, 1999.
- [5] Gary R. Ferries and R. Larry Arbanas, "Control/Structure Interaction in Hydraulic Power Steering System," June, 1997, AACC
- [6] J. M. Smith, G. R. Ferries and R. L. Arbanas, "An Analytical Systems Approach to Steering Shudder," Proceedings of the 1995 SAE Noise and Vibration Conference, 1995. P-291, pp. 151-155.
- [7] A. Zarembo and R. I. Davis, "Dynamic Analysis and Stability of a Power Assist Steering System," Proceedings of the ACC, June, 1995.
- [8] Ali Y. Orbak, Kamal Youcef-Toumi and Masaaki Senga, "Model Reduction and Design of a Power Steering System," Proceedings of the ACC, June, 1999.
- [9] Ali Y. Orbak and Kamal Youcef-Toumi, "Model reduction in the Physical Domain," MIT report. Department of Mechanical Engineering, 1998.
- [10] Aly Badawy, J. Zuraski, F. Bolourchi and A. Chandy, "Modelling and Analysis of an Electric Power Steering System," SAE technical paper, 1999-01-0399.
- [11] Manu Parmar and John Y. Hung, "Modelling and Sensorless Optimal Controller Design for an Electric Power Assist Steering System," IEEE, 2002.
- [12] Tankut Acarman, Keith A. Redmill and Umit Ozguner, "A Robust Controller Design for Drive by Wire Hydraulic Power Steering System," Proceedings of the ACC, May, 2002

- [13] A. T. Zaremba, M. K. Liubakka and R. M. Stuntz, "Control and Steering Feel Issues in the Design of an Electric Power Steering System," Proceedings of the ACC, June, 1998.
- [14] J. Baxter, "Analysis of stiffness and feel for a Power-Assist Rack and Pinion Steering Gear," SAE paper, 880706, 1988.
- [15] F. J. Adams, "Power Steering Road Feel," SAE paper, 830998, 1983.
- [16] J. Engelman, "A System Dynamic Perspective on Steering Feel," Ford Motor Company Research Report, May, 1994.
- [17] R. McCann, L. R. Pujara, J. Lieh, "Influence of Motor Drive Parameters on the Robust Stability of Electric Power Steering Systems," Power Electronics in Transportation, IEEE conference paper, Oct., 1998.
- [18] S. V. Gusev and A. T. Zaremba, "LMI based minimax control under component-wise constraints on the input with the application to an electric power steering system," Proceedings of the 38th CDC, December, 1999.
- [19] J. Y. Wong and D. P. Looze, "Robust performance for system with component-wise signal," Automatica, 31, 471-475, 1995.
- [20] R. D'Andrea, " H_∞ optimization with spatial constraints," Proceedings of the 34th CDC, 4327-4332, 1995.
- [21] S. V. Gusev, "Minimax control under a constraint on the moments of disturbance," Proceedings of the 34th CDC, 1195-1200, 1995.
- [22] S. V. Gusev, "Method of moment constrictions in robust control and filtering," Proceedings of the 13th IFAC world congress, 415-420, 1996.
- [23] S. V. Gusev, W. Johnson and J. Miller, "Active Flywheel Control Based on the Method of Moment Restrictions," Proceedings of the ACC, Vol. 5, 3426-3430, 1997.
- [24] S. Boyd, L. El. Ghaoui, E. Feron and V. Balakrishnan, "Linear Matrix Inequalities in Systems and Control Theory," Philadelphia, PA: SIAM, 1994.
- [25] Y. Nesterov, V. Nemirovski, "Interior point Polynomial Methods in Convex Programming: Theory and Applications," Philadelphia, PA: SIAM, 1994.
- [26] P. Gahinet, A. Nemirovski, A. J. Loub and M. Chilali, "LMI Control Toolbox," User's guide, MathWorks, Inc.

- [27] M. Chilali and P. Gahinet, "H_∞ design with pole placement constraints: an LMI approach," IEEE transaction on Automation and Control, AC-41, 358-367, 1996.
- [28] C. Scherer, P. Gahinet and M. Chilali, "Multiobjective Output feedback control via LMI Optimization," IEEE transaction on Automatic Control, AC-42, 896-911, 1997.
- [29] M. Kurishige and T. Kifuku, "Static Steering-Control system for Electric-Power Steering," technical paper, Mitsubishi Electric Advance, June, 2001.
- [30] D. G. Luenburger, "Observing the state of linear system," IEEE transaction, Mil. Electron, 1964.
- [31] J. B. Burl, "Linear Optimal Control, H₂ and H_∞ Methods," Addison Wesley Longman Inc., 1999.
- [32] S. Endo, "Control Apparatus with Stability Compensator for Electric Power Steering System," 5,732,373, US Patent.
- [33] H. Kawada, Y. Itakura and T. Sakaguchi, "Control Unit for Electric Power Steering Apparatus," 6, 381, 528, B1, US Patent.
- [34] "Steering – Electronic Power Assist," SG2010/D, REV 0, Motorola Reference Design, Dec., 2002.
- [35] K. Zhou, J. C. Doyle and K. Glover, "Robust and Optimal Control," Prentice Hall, Upper Saddle River, New Jersey, USA, 07458.
- [36] J. M. Maciejowski, "Multivariable Feedback Design," Workingham: Addison-Wesley.
- [37] G. Zames, "Feedback and optimal sensitivity: model reference transformations, multiplicative seminorms, and approximate inverses," IEEE transaction on Automatic Control, vol. AC-26, pp. 301-320, 1981.
- [38] J. C. Doyle, "Lecture notes in advances in multivariable control," ONR/Honeywell Workshop, 1984.
- [39] K. Glover, "All optimal Hankel-norm approximations of linear multivariable systems and their L_∞-error bounds," Int. J. Control, vol. 39, pp. 1115-1193, 1984.
- [40] K. Glover and J. Doyle, "State-space formulae for all stabilizing controllers that satisfy an H_∞ norm bound and relations to risk sensitivity," Systems and Control Letters, vol. 11, pp. 167-172, 1988.

- [41] I. R. Petersen, "Disturbance attenuation and H_∞ optimization: a design method based on the algebraic Riccati equation," IEEE Transaction on Automatic Control, vol. AC-32, pp. 427-429, 1987.
- [42] K. Zhou and P. P. Khargonekar, "An algebraic Riccati equation approach to H_∞ optimization," Systems and Control Letters, vol. 11, pp. 85-92, 1988.
- [43] I. Chikuma, "Electric Power Steering System," 5,454,438, US patent.
- [44] "CarSim User Manual Version 5.11," Mechanical Simulation Corporation, 709 West Huron, Ann Arbor, MI 48103.
- [45] R. Chiang, M. Safonov, "Robust Control Toolbox, for use with MatLab®," the MATHWORKS Inc.
- [46] M. G. Safonov, D. J. N. Linmebeer and R. Y. Chiang, "Simplifying the H_∞ Theory via Loop Shifting, Matrix Pencil and Descriptor Concepts," Int. J. Control, 50, 6, pp. 2467-2488, 1989.
- [47] N. Sugitani, Y. Fujiwara, K. Uchida, M. Fujita, "Electric Power Steering with H-infinity Control Designed to Obtain Road Information," Proc. of the ACC. June, 1997.

VITA AUCTORIS

NAME: Ke Li

PLACE OF BIRTH Beijing, China

YEAR OF BIRTH 1974

EDUCATION Beijing Experimental Middle School, Beijing, China
1990-1993

Beijing University of Posts and Telecommunications
1993-1997 B.Sc

University of Windsor, Windsor, Ontario
2002-2004 M.Sc